Geophysical Journal International

Geophys. J. Int. (2010) doi: 10.1111/j.1365-246X.2010.04766.x

From the Variscan to the Alpine Orogeny: crustal structure of the Bohemian Massif and the Western Carpathians in the light of the SUDETES 2003 seismic data

P. Hrubcová,[1] P. Środa,[2] M. Grad,[3] W. H. Geissler,[4] A. Guterch,[2] J. Vozár,[5] E. Hegedűs[6] and Sudetes 2003 Working Group

[1]*Institute of Geophysics, Academy of Science of the Czech Republic, Boční* II/1401, 141 31 *Prague* 4, *Czech Republic. E-mail: pavla@ig.cas.cz*
[2]*Institute of Geophysics, Polish Academy of Sciences, Ks. Janusza* 64, 01-452 *Warsaw, Poland*
[3]*Institute of Geophysics, University of Warsaw, Pasteura* 7, 02-093 *Warsaw, Poland*
[4]*Alfred Wegener Institute for Polar and Marine Research, Am Alten Hafen* 26, D3210, D-27568 *Bremerhaven, Germany*
[5]*Slovak Academy of Sciences, Geological Institute, Bratislava, Slovak Republic*
[6]*Eötvös Loránd Geophysical Institute, Budapest, Hungary*

Accepted 2010 August 6. Received 2010 July 15; in original form 2010 January 12

SUMMARY

The Variscan orogeny is the major Middle to Late Palaeozoic tectonometamorphic event in central Europe, and the Bohemian Massif is the largest exposure of rocks deformed during this orogeny. The Bohemian Massif consists of the Saxothuringian, Barrandian and Moldanubian units. Adjacent to this massif in the southeast, the Western Carpathians form an arc-shaped mountain range related to the Alpine orogeny during the Cretaceous to Tertiary. The complex crustal-scale geological structure of the Variscan Bohemian Massif and the Western Carpathians, and especially their contact, were analysed in this study employing the data of the SUDETES 2003 international seismic refraction experiment. The analysed seismic data were acquired along the 740 km long, NW–SE oriented S04 profile that crossed the Bohemian Massif and the Western Carpathians before terminating in the Pannonian Basin. The data were interpreted by 2-D trial-and-error forward modelling of *P* waves, and additional constraints on crustal structure were provided by gravity modelling.

The complex velocity structure derived in our analysis included low velocities of 5.85 km s^{-1} at the contact of the Saxothuringian and Barrandian units that reflect the presence of low-density granites. There are distinct lateral variations in deep crustal structure in the transition between the Bohemian Massif and the Western Carpathians. The abrupt change of the crustal thickness in this transition zone may be associated with the Pieniny Klippen Belt, a deep-seated boundary between the colliding Palaeozoic lithospheric plate to the north and the ALCAPA microplate to the south. In the upper crust of this transition, low velocities of 4 km s^{-1} extend to 6 km and represent the sedimentary fill of the Carpathian Flysch and Foredeep that thins towards the foreland. This basin is also expressed as a pronounced gravity low. The Moho in the Carpathians reaches a depth of 32–33 km. In contrast, in the Pannonian Basin the Moho rises to a depth of 25 km, which corresponds to the Pannonian gravity high.

Key words: Controlled source seismology; Body waves; Continental margins: convergent; Crustal structure; Europe.

1 INTRODUCTION

The Variscan orogeny is the major Middle to Late Palaeozoic tectonometamorphic event in central Europe. It represents the final collision of Gondwana with the northern continent, Laurasia, and marks the European version of the evolution of the supercontinent of Pangaea at the end of the Palaeozoic (McCann 2008a). During the Cretaceous to Tertiary, the post-Variscan stage was followed by extensional and compressional tectonics, related to plate motions between Europe and Africa, which resulted in the Alpine orogeny. The largest Variscan unit in central Europe, the Bohemian Massif, represents the most prominent outcrop of pre-Permian rocks. It was formed by the amalgamation of individual Armorican terranes and their final collision with Avalonia and the western margin of the Brunovistulian (Schulmann & Gayer 2000). Further to the SE, the Western Carpathians form an arc-shaped mountain range originating as a result of the convergence of the European and African plates since the Late Jurassic through Quaternary (McCann 2008b).

As follows, the region is a complex of tectonic units ranging from Cadomian to Tertiary age with Variscan to Alpine tectonics. In an effort to investigate such a structure, central Europe has been covered by a network of seismic refraction experiments (POLONAISE'97, CELEBRATION 2000, ALP 2002 and SUDETES 2003) as a result of a massive international cooperative effort (Guterch *et al.* 1998, 1999, 2003a,b; Brückl *et al.* 2003; Grad *et al.* 2003a,b). This paper focuses on the refraction and wide-angle reflection experiment SUDETES 2003, which involved a consortium of European and North American institutions comprising geophysical groups from the Czech Republic, Poland, the United States, Germany, Slovakia and Hungary. In this study, we present a detailed analysis of the data from the main SUDETES 2003 profile S04 (Figs 1 and 2) that extends NW to SE from Germany, across all main tectonic units of the Bohemian Massif and continues through the Western Carpathians to the Pannonian Basin in Hungary.

The complex geological structures of the Variscan Bohemian Massif and the Western Carpathians, and especially their contact, are not completely understood or solved in many aspects and are subject to ongoing research and debate. The Bohemian Massif is an excellent example of the Variscan crust exposed to the surface, whereas the Carpathian crust records the crust-forming processes during the Mesozoic to Cenozoic. The S04 profile is in a favourable position for studying the individual tectonic units within the Bohemian Massif. Above, its prolongation across the Western Carpathian arc provides an opportunity to study this orogenic belt as well as its contact with the Bohemian Variscan units in the NW. The interpretation of the S04 data provides a new insight into the deep structure and superposition of the tectonic units at depth. Contrasts in seismic properties together with the depth of the Moho discontinuity reflect compositional and structural variances resulting from crust-forming processes during Cadomian, Palaeozoic and Tertiary tectonic development.

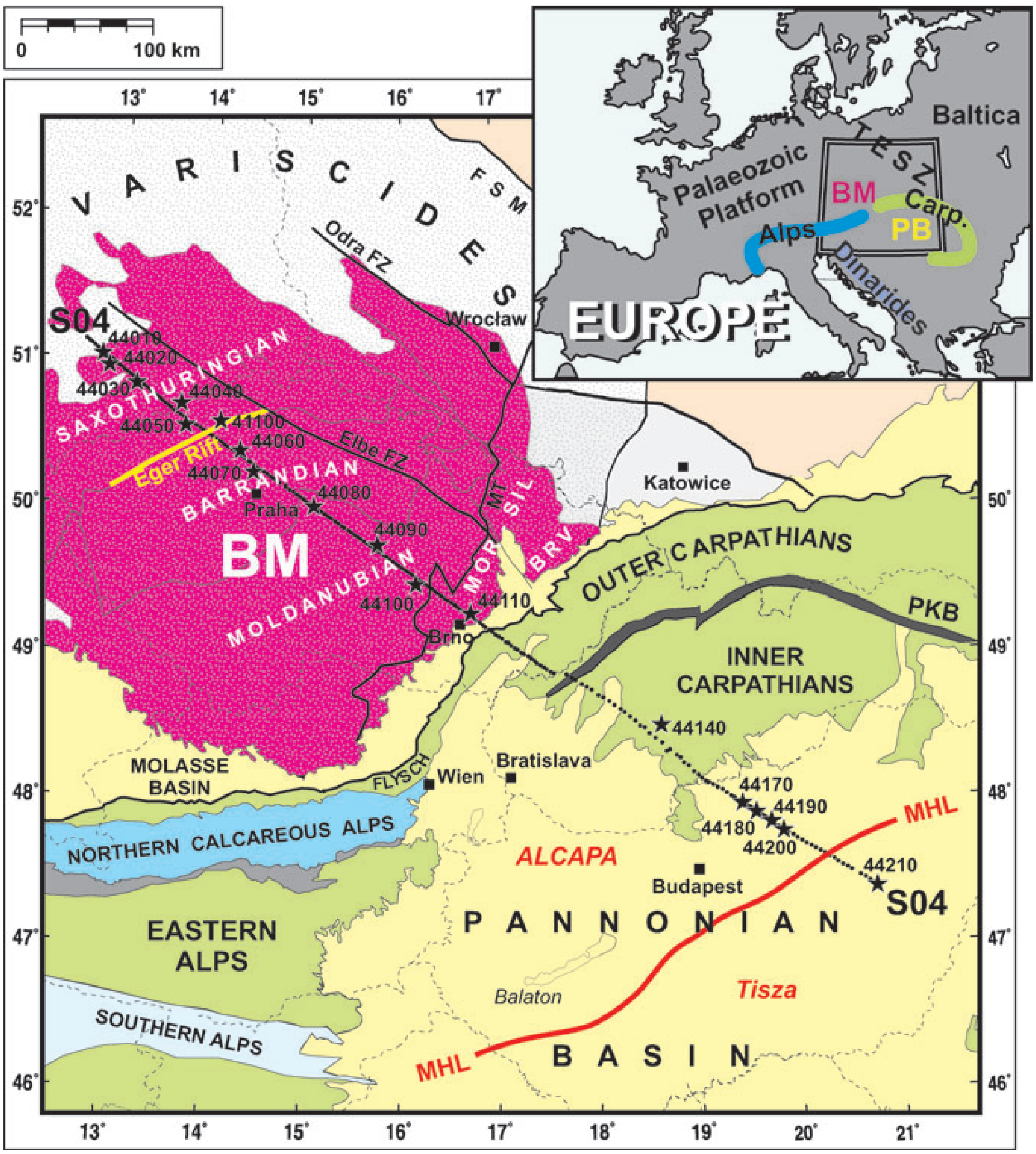

Figure 1. Location of the S04 profile superimposed on a simplified tectonic map. The insert shows major tectonic units in central Europe. BM, Bohemian Massif; PB, Pannonian Basin; Carp., Carpathians; TESZ, Trans-European Suture zone; Mor-Sil, Moravo-Silesian; Brv, Brunovistulian; MT, Moldanubian Thrust; PKB, Pieniny Klippen Belt; MHL, Mid-Hungarian Line.

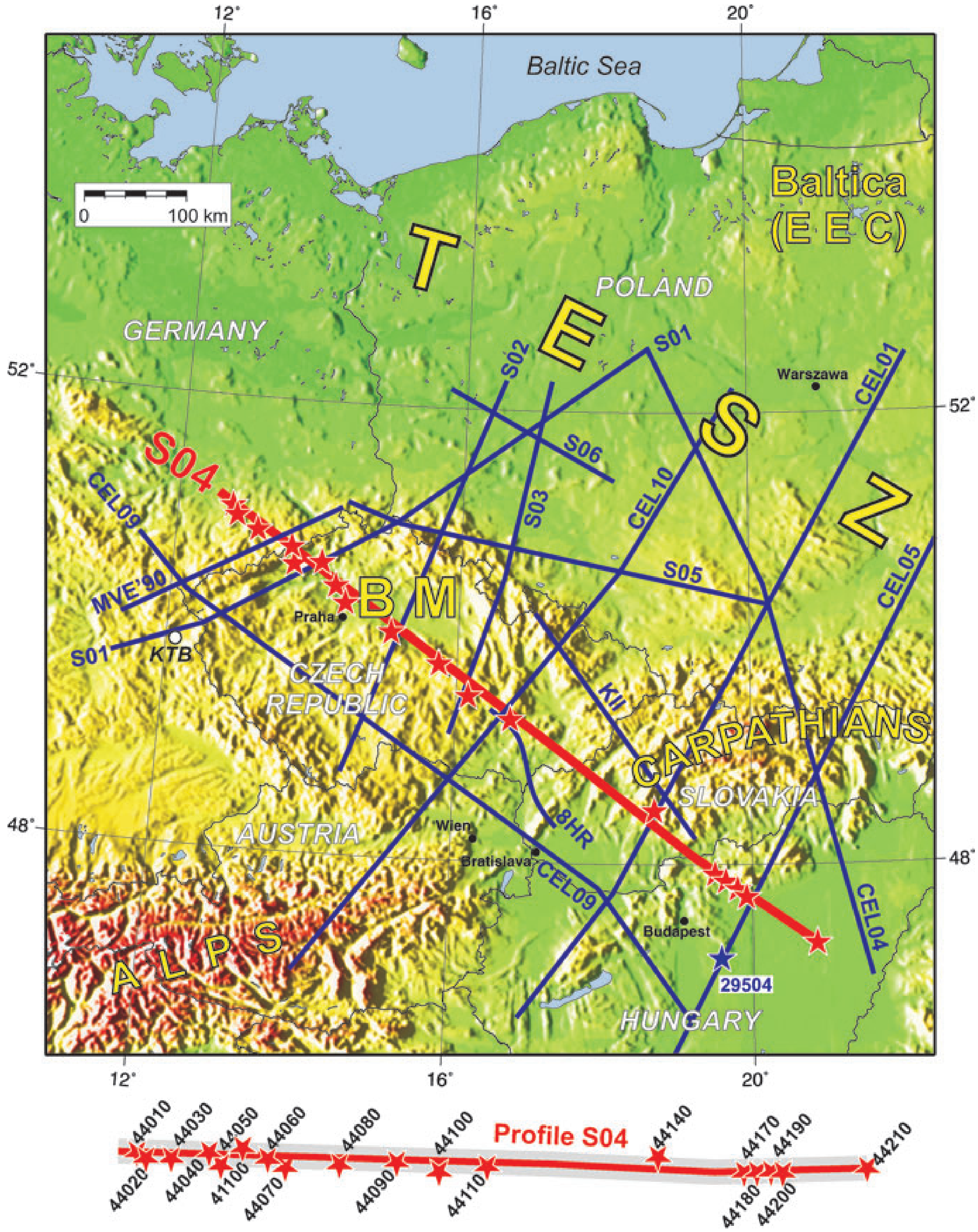

Figure 2. Location of the S04 profile with the shot numbers. Stars mark the positions of individual shot points, the red line refers to the recording positions. Other seismic refraction and reflection profiles (CELEBRATION 2000—CEL01, CEL04, CEL05, CEL09, CEL10; SUDETES 2003—S01, S02, S03, S05, S06; MVE-90 and 8HR) are indicated by dark blue solid lines. Blue star refers to the shot point SP 29504 of the CEL09 line. White circle shows the location of the KTB deep borehole. The shots along the S04 profile with their numbers are shown at the bottom of the figure. BM, Bohemian Massif; TESZ, Trans-European Suture zone; EEC, East European Craton.

2 GEOLOGY AND TECTONIC EVOLUTION OF THE REGION

The eastern termination of the Variscan belt in central Europe comprises the Bohemian Massif, which developed approximately between 480 and 290 Ma (Matte 2001) during a period of large-scale crustal convergence, collision of continental plates and microplates and subduction (Matte *et al.* 1990). It includes the formation of the cratonic basement, Cadomian orogenic processes and variable reworking during the Variscan orogeny. In places the massif underwent the highest known Variscan metamorphic overprint, while other units of the massif show only a very low grade tectonometamorphic overprint and well-preserved remnants of the Cadomian basement and its Early Palaeozoic overstep sequences. The Bohemian Massif consists mainly of low- to high-grade metamorphic and plutonic Palaeozoic rocks and can be subdivided into several tectonostratigraphic units: the Saxothuringian, the Barrandian, the Moldanubian and the Moravo-Silesian, separated by faults, shear zones or thrusts (Fig. 1).

The Moldanubian unit represents a major crystalline segment within the Bohemian Massif and its boundary with the Saxothuringian in the NW is regarded to be a suture-type discontinuity. A structurally higher unit, the Barrandian, has been thrust over the Saxothuringian rocks towards the northwest (Dallmeyer *et al.* 1995). Reactivation of crustal-scale shear zones during the mid-Cretaceous led to the formation of the Bohemian Cretaceous Basin along the NW–SE oriented Elbe Fault Zone reflecting a large-scale zone of crustal weakness. Later, this area was affected by Permo-Carboniferous post-orogenic extension, as well as alkaline magmatism during the Cenozoic evolution of the Eger Rift, a geodynamically active zone belonging to the European Cenozoic Rift System (Prodehl *et al.* 1995).

The Moldanubian/Moravian boundary in the east has the character of a ductile shear zone with a significant translation of the Moldanubian over the Moravian unit during a final stage of the subduction of the oceanic crust and subsequent Variscan collision between the Moldanubian terrane and the Brunovistulian microcontinent to the east (Dudek 1980). In this event, the Moldanubian is viewed as a Variscan orogenic root thrust over the Brunovistulian forming together the Moravo-Silesian zone (Matte 1991; Schulmann *et al.* 2005). The Moravian unit consists of a Cadomian basement, the Brunovistulian, covered by Devonian to Carboniferous sediments and submerging to the east beneath the Carpathian Foredeep, where it forms the basement reactivated during the Alpine orogeny (Schulmann & Gayer 2000). In the Mesozoic, the area was subject to platform development and rifting along the southern/southeastern flank of the Bohemian Massif.

The Western Carpathians form a northward-convex arc as a result of a series of Jurassic to Tertiary subduction and collision events. They represent the northernmost part of the Alpine belt, which evolved during the Alpine orogeny. The geological evolution of the individual parts is rather complicated, comprising tectonic processes such as folding, thrusting and the formation of sedimentary basins of various types in the Mesozoic and Tertiary. These processes resulted in the superposition of the Variscan high-grade crystalline basement and its Late Palaeozoic and Mesozoic cover, overridden by superficial nappe systems and post-nappe cover formed by the Palaeogene, Neogene and Quaternary rocks. Like most of the other collisional fold-belts, the Western Carpathians have been divided into the outer and inner zones based largely on the relative ages of the Alpine events and the intensity of their deformation and metamorphic effects (McCann 2008b).

The Outer Western Carpathians include the Carpathian Foredeep, the eastern prolongation of the Alpine Molasse Basin and the Carpathian Flysch Belt, a Tertiary accretionary complex composed of several north to north-west-verging nappes. They are thrust over the Carpathian Foredeep filled by Neogene strata. The Inner Western Carpathians, covering most of Slovakia, include various pre-Tertiary units and unconformable Cenozoic sedimentary and volcanic complexes. They are followed by isolated mountains in northern Hungary comprising mainly unmetamorphosed Palaeozoic and Mesozoic complexes covered by deposits of the Late Cretaceous, Palaeogene and Early Neogene intermontane basins up to 3.5 km thick (Plašienka *et al.* 1997; Janočko & Jacko 1999; Soták *et al.* 2001).

From a tectonic point of view, the Outer Western Carpathians correspond to a Tertiary accretionary complex related to the southward subduction of the oceanic to suboceanic crust. They are separated from the Inner Western Carpathians by the Pieniny Klippen Belt, a deep-seated boundary between the colliding Palaeozoic lithospheric plate and the microplate ALCAPA. The Pieniny Klippen Belt forms a narrow zone of extreme shortening and wrenching between the accretionary wedge and the Inner Western Carpathians representing the backstop (Birkenmajer 1986). According to this interpretation, during the Tertiary the Carpathian Foredeep was a peripheral foredeep formed due to regional flexure of the descending plate (Krzywiec 1997). The subduction-related nappe stacking in the Outer Western Carpathians was followed by regional collapse resulting in the formation of intermontane basins filled by Neogene and Quaternary strata (Zuchiewicz *et al.* 2002).

In the south, the Western Carpathian area also includes the subsurface of the wide flat lowlands of the Pannonian Basin (Horváth 1993; Tari *et al.* 1993). The Pannonian Basin System is filled by more than 2 km of Palaeogene and up to 7 km of Neogene and Quaternary sedimentary cover (Royden *et al.* 1983). It was formed within the Inner Carpathians and the Tisza unit due to back-arc stretching and mantle upwelling (Konečný *et al.* 2002).

3 PREVIOUS GEOPHYSICAL INVESTIGATIONS IN THE STUDY AREA

The first attempts to reveal the crustal structure of this vast region were associated with the investigation of the Bohemian Massif (Beránek & Zátopek 1981) or with the investigation of the Carpathian Foreland (Majerová & Novotný 1986; Bielik *et al.* 2004). The interpretation of the refraction measurements indicated a pronounced Moho discontinuity in the central part of the Bohemian Massif with a maximum depth of 39 km and a less pronounced, sometimes blurred, Moho at a depth of about 32 km at the eastern margin of the Bohemian Massif at its contact with the Carpathians (Beránek & Zounková 1977). These measurements were complemented by reflection profiling, as well as by other geophysical methods (see Bucha & Blížkovský 1994).

More detailed results were obtained from the refraction and wide-angle reflection experiments CELEBRATION 2000, ALP 2002 and SUDETES 2003 (Málek *et al.* 2001; Růžek *et al.* 2003, 2007; Grad *et al.* 2003b; Guterch *et al.* 2003a,b; Hrubcová *et al.* 2005, 2008; Środa *et al.* 2006; Brückl *et al.* 2007) (Fig. 2), which followed previous seismic studies in central Europe (Guterch *et al.* 1999; Grad *et al.* 2002, 2003a, 2006). Two perpendicular profiles, CEL09 and CEL10, crossing the whole Bohemian Massif provided new information about the structure and particularly about the lower crustal properties and the character of the crust–mantle transition. A highly reflective lower crust was associated with the Saxothuringian in the NW, the deepest and the most pronounced Moho was detected in the Moldanubian and a broad crust–mantle transition zone along the eastern edge of the Bohemian Massif (Hrubcová *et al.* 2005, 2008). SUDETES 2003 profile S01 provided a good regional picture on the lithospheric structure along the Eger Rift (Grad *et al.* 2008); profiles S02 and S03 gave an insight of the Bohemian Massif in the north–south direction (Majdański *et al.* 2006, 2007). In SE Germany, the seismic refraction and wide-angle reflection profile GRANU'95 (Enderle *et al.* 1998) showed the velocity structure of the Saxothuringian belt. A laminated lower crust was indicated by the deep reflection profile MVE-90 as a part of the DEKORP investigations (DEKORP Research Group 1994) and during a combined investigation of the refraction and receiver function data (Hrubcová & Geissler 2009).

An important contribution to the understanding of the geological structure at the transition between the Bohemian Massif and the

Carpathians was provided by the interpretation of the regional refraction profile KII extending from the border of the Czech Republic and Poland to Slovakia. In the Silesian zone, two bands of reflections suggested that the Moho is located at a depth of 36–37 km and rises towards the SE to 30–32 km (Majerová & Novotný 1986). The deep seismic reflection profile 8HR further to the south (Fig. 2), close to the S04 profile, indicated the Moho at a depth of 35–37 km.

The Carpathian Mountains and their foredeep were also subject to the early deep seismic sounding studies, which resulted in a crustal thickness of 40 km. Later, these measurements were complemented by reflection profiling (Tomek 1993; Tomek & Hall 1993; Vozár *et al.* 1999; Šantavý & Vozár 2000), as well as by the detailed refraction and wide-angle reflection experiment CELEBRATION 2000 (Grad *et al.* 2006; Malinowski *et al.* 2005, 2008). Profiles CEL01, CEL04 and CEL05 crossed the Carpathian arc in the N–S direction and gave an insight into the main tectonic features associated with the Carpathians and the Pannonian Basin System (Grad *et al.* 2006; Środa *et al.* 2006). In the Pannonian Basin, both refraction and deep reflection profiles recorded since 1970 revealed a thinner crust of about 25–30 km and a low-velocity layer in the upper mantle, the top of which is at a depth of 55 km (Posgay *et al.* 1981, 1986, 1995).

Seismic investigations were complemented by other geophysical methods, especially gravity measurements. The gravitational field pattern of the Bohemian Massif is divided into four positive and negative regional bands running SW–NE (Bucha & Bližkovský 1994). They are perpendicular to the S04 profile with a minimum of −60 mGal near the contact of the Saxothuringian and Barrandian at the Eger Rift related to granitic rocks. The Carpathian gravity low is attributed to low-density porous foredeep sediments covered by nappes of the Outer Western Carpathian accretionary wedge. The Pannonian gravity high results from a significantly shallower Moho (Bielik *et al.* 2004).

4 SEISMIC DATA

4.1 Acquisition and processing

The data along the refraction and wide-angle reflection profile S04 were acquired during the international seismic experiment SUDETES 2003 (Grad *et al.* 2003). This experiment took place mainly in the Czech Republic and Poland but also covered portions of Germany, Slovakia and Hungary. Its NW–SE oriented transect S04 was the longest profile of the SUDETES 2003 experiment and started at the north-west edge of the Bohemian Massif in the Saxothuringian, crossed the Eger Rift, continued along the northern rim of the Barrandian and Moldanubian to the Moravo-Silesian. It then continued across the Carpathian Foredeep and Flysch Belt to the Western Carpathians and terminated in the Pannonian Basin. The S04 profile was 740 km long with 18 shot points, of which one was fired twice. About 250 single-channel recorders were deployed along the S04 profile; all recorders were of the Texan type (RefTek 125, Refraction Technology Inc., Plano, TX, USA) and employed 4.5 Hz vertical geophones. The average distance between the shots was 30 km with an average station spacing of 3 km in the Czech Republic and Germany and 4 km in Slovakia and Hungary. A few stations in Hungary near the Matra Mts. (distance of 610–650 km along the profile) were deployed with a denser spacing of less than 1 km for shallow structure study. The charges amounted to 400 kg on average. For three shot points larger charges were used. The positions of shot points and stations were measured by GPS; the origin time was controlled by a GPS-controlled blasting device. Fig. 2 shows the field layout of the SUDETES 2003 seismic experiment; for more details on geometry refer to Grad *et al.* (2003) and Guterch *et al.* (2003). The shots along the S04 profile with their numbers are shown at the bottom of Fig. 2 and detailed information about the shots is presented in Table 1.

The data from the experiment were recorded with a sampling rate of 0.01 s with a recording time window of 300 s for each shot. Data processing included bandpass filtering of the whole data set (usually 2–15 Hz) to remove low- and high-frequency noise. Recordings were sorted into shot gathers; seismic sections were trace-normalized to the maximum amplitude along the trace and cut to a length of 100 s starting at zero reduced time. They were plotted with a reduction velocity of 8 km s^{-1}, a velocity of the upper mantle commonly used for data visualisation in crustal/upper mantle studies. For plotting, the seismic sections were cleaned and bad quality (noisy) traces (or their parts) were removed. Examples of the recorded wavefields are shown in Fig. 3.

4.2 Seismic wavefield

The seismic data used for the interpretation along the S04 profile have a good signal-to-noise ratio for the *Pg* phases as the refractions

Table 1. Details of the explosive sources along the S04 profile of the *SUDETES 2003* experiment.

Shot number	Longitude (°E)	Latitude (°N)	Date (dd/mm/yyyy)	Time UTC (hh:mm:ss.sss)	Charge (kg)
44010	12.762560	51.022500	06/06/2003	08:01:00.000	30
44020	12.836900	20.945500	06/06/2003	16:01:00.000	1000
44030	13.143900	50.829500	06/06/2003	12:16:22.680	425
44031	13.143000	50.829000	06/06/2003	12:25:22.929	2930
44040	13.635666	50.697000	04/06/2003	19:00:00.624	400
44050	13.687163	50.548466	04/06/2003	18:49:59.990	400
44060	14.282000	50.378666	04/06/2003	19:20:00.689	400
44070	14.428166	50.234000	05/06/2003	03:50:00.029	260
44080	15.079601	49.998864	05/06/2003	18:09:59.513	400
44090	15.760150	49.734280	04/06/2003	17:50:01.843	400
44100	16.165500	49.463500	06/06/2003	03:11:15.778	400
44110	16.744416	49.266916	06/06/2003	03:50:01.183	400
44140	18.704250	48.474333	07/06/2003	04:30:00.119	400
44170	19.507500	47.916400	06/06/2003	01:20:00.000	350
44180	19.645800	47.849700	06/06/2003	02:20:00.000	60
44190	19.796100	47.780600	07/06/2003	01:20:00.000	60
44200	19.915500	47.714700	07/06/2003	02:20:00.000	60
44210	20.834400	47.301900	05/06/2003	01:40:00.000	700

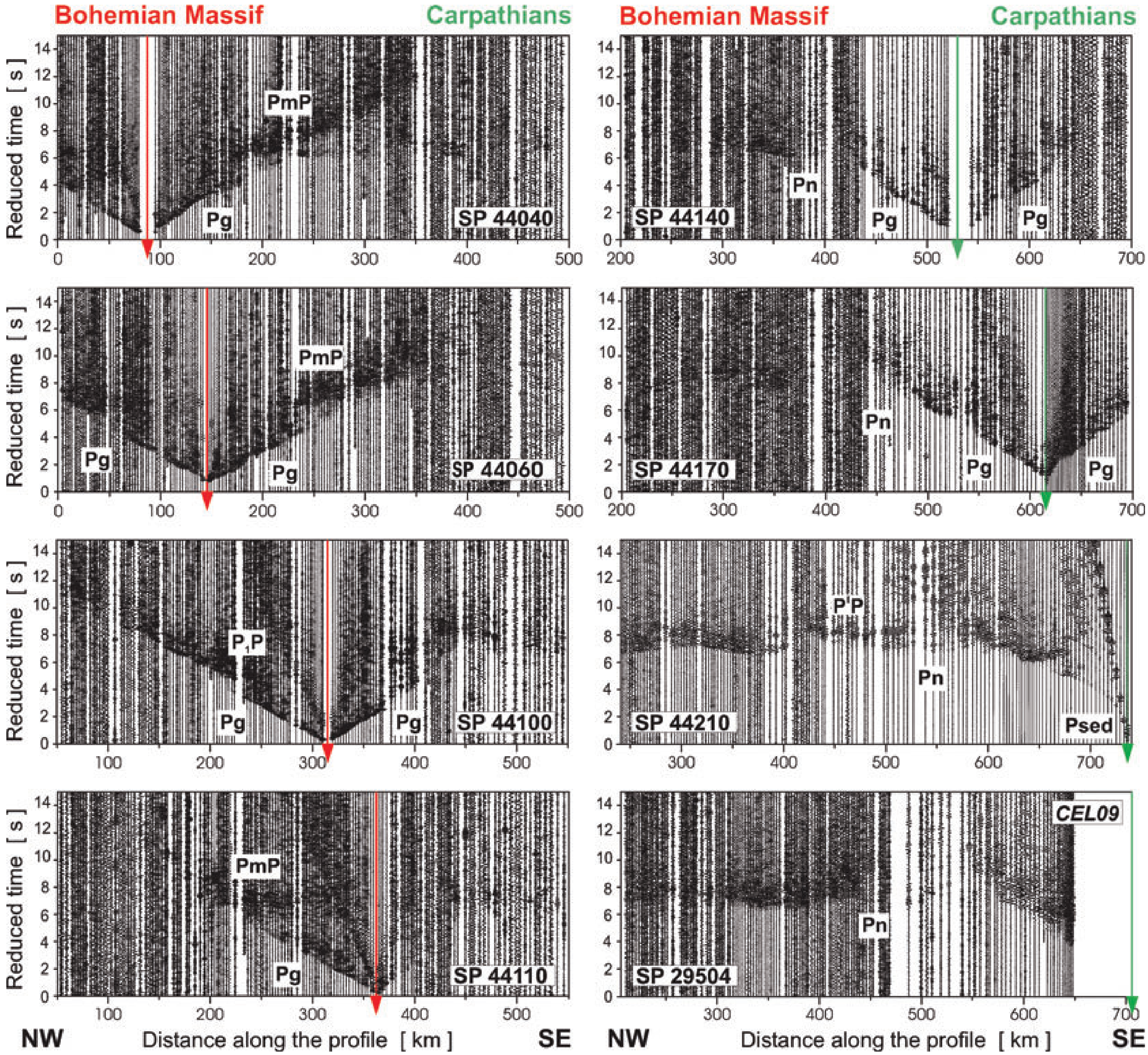

Figure 3. Examples of amplitude-normalized vertical component seismic sections from different parts of the S04 profile plotted with reduction velocity of 8 km s^{-1}. (Left panel) Shot points in the Bohemian Massif (red arrows). (Right panel) Shot points in the Carpathians (green arrows). Seismic section from SP 29504 in the Carpathians along the CEL09 profile (see Fig. 2, bottom right). Note differences in the energy propagation in the SE and NW directions, where shot points in the Bohemian Massif show an abrupt termination of energy in the southeast direction at the contact with the Carpathians (distance of 400 km along the profile). In contrast, data recorded in the northwest direction from reciprocal shot points in the Pannonian Basin show the energy up to offsets of more than 500 km (SP 44210, SP 29504).

from the upper crust, and the *PmP* phases as the reflections from the Moho discontinuity. The *Pn* waves refracted from the upper mantle are sometimes not well developed and are only visible on a few record sections. Refracted waves from the sedimentary cover (*Psed* phases) are observed in the vicinity of shot points mainly in the SE in the Pannonian Basin. Other phases are complex and sometimes difficult to pick and correlate among shot points. This fact concerns intracrustal reflections P_1P, and upper mantle reflections P^IP.

Clear arrivals of refracted waves from the crystalline crust (*Pg* phase) are typically observed up to offsets of 100–120 km. In the area of the Bohemian Massif, they show an apparent velocity of 5.8–6.1 km s^{-1}. Short-wavelength anomalies of the *Pg* phase reflect the existence of near surface velocity inhomogeneities. Lower apparent velocities of about 5.5–5.75 km s^{-1} correlate with the sedimentary basin of the Barrandian unit (the Most Basin at 145 km along the profile) and southern margins of the Bohemian Cretaceous Basin (at about 200 and 280 km along the profile) located along the NW–SE oriented Elbe Fault Zone.

In the middle part of the profile, at the contact of the Bohemian Massif with the Carpathians, there are strong differences in the wavefields. The shot points in the Bohemian Massif (Fig. 3—SP 44100 and SP 44110) show an abrupt termination of energy for all phases in the southeast direction from a distance of 400 km along the profile. In contrast, data recorded in the northwest direction from

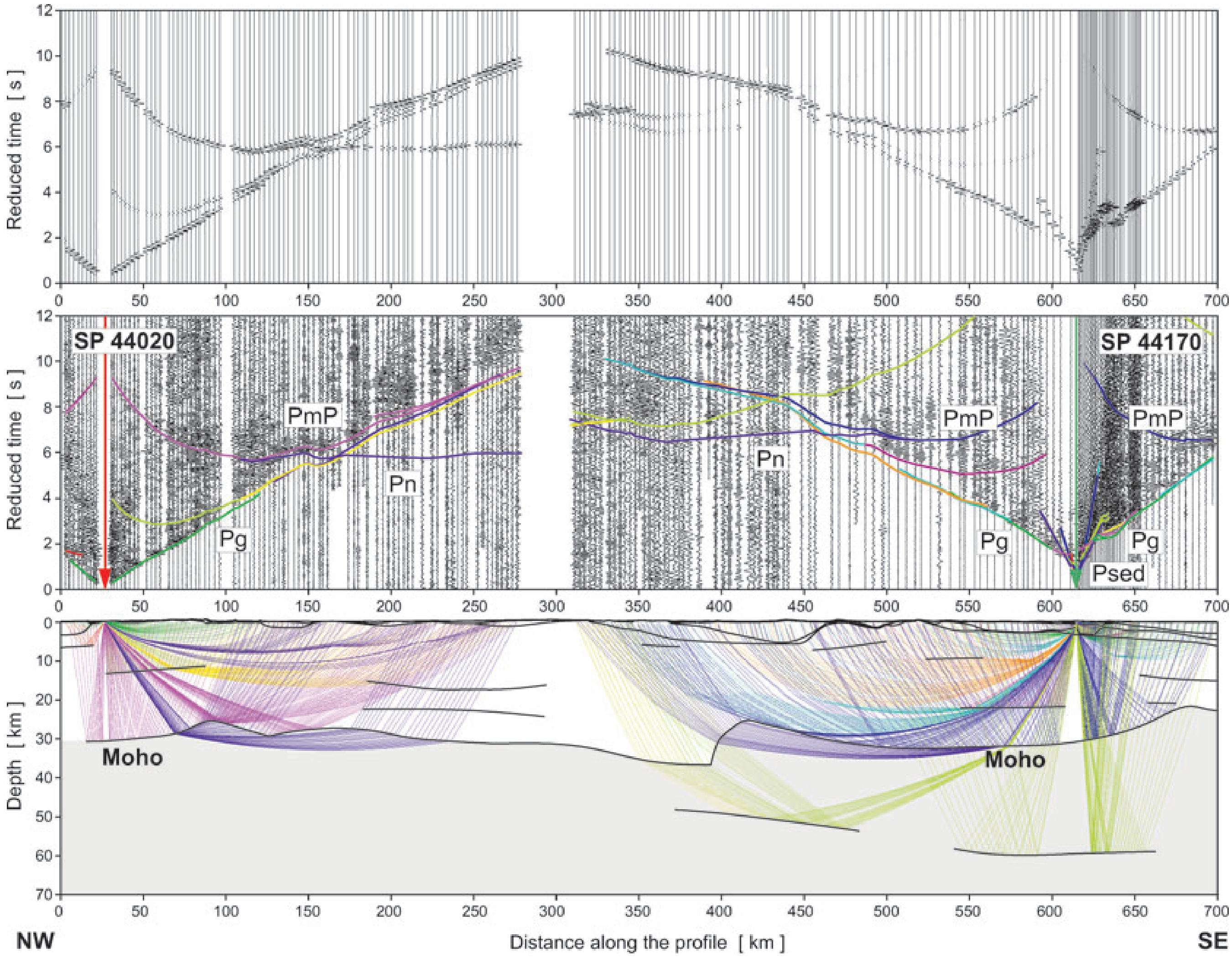

Figure 4. Examples illustrating forward modelling in the Bohemian Massif—the Saxothuringian (SP 44020) and the Carpathians (SP 44170). For both shot points: (top panel) synthetic seismic sections, (middle panel) amplitude normalized record sections with theoretical traveltimes and (bottom panel) model and ray paths calculated for the final model (Fig. 5) using the *SEIS83* ray tracing technique. Data have been bandpass filtered from 2 to 15 Hz. Reduction velocity is 8 km s^{-1}. Identification of main seismic phases: *Pg*, refraction within the crust; *Pn*, refraction from the uppermost mantle; *PmP*, reflection from the Moho discontinuity; *Psed*, refraction within sediments.

reciprocal shot points in the Pannonian Basin (Fig. 3—SP 44210 and SP 29504) display energies up to offsets of more than 500 km (recorded up to the Barrandian of the Bohemian Massif to a distance of 200 km along the profile). This effect is visible not only in the SUDETES 2003 data but also in the CELEBRATION 2000 data in the same area and reflects strong damping in the upper crust of the Carpathian Flysch and in the nappes of the Inner Carpathians observed in the SE direction. A similar effect was also visible in some sections of the CELEBRATION 2000 experiment along the profiles CEL01, CEL04 and CEL05 in the area of the same tectonic unit (Grad *et al.* 2006; Środa *et al.* 2006). There are two reasons explaining this effect. First, the attenuation of energy is due to porous material of the Carpathian Foredeep and Flysch in the upper crust. When the energy penetrates deeper into the crust and mantle it can propagate well because the damping is mainly constrained to the upper crustal levels. Another reason might be the direction of the energy recording. When recorded to the SE, the energy is damped while when recorded in the opposite direction, to the NW, the energy is visible even for the upper crust as is seen in the data from SP 44140 or SP 44170 in the Carpathians (Fig. 3—SP 44140 and SP 44170, Fig. 4—SP 44170). This may thus be a response due to the direction of the northwest-ward Carpathian nappe thrusting.

In the SE, the first arrivals at offsets smaller than 30 km display an apparent velocity of 2.5–5 km s^{-1} for the shot points of SP 44170, SP 44180, SP 44190 and SP 44200 and especially SP 44210. This reflects a few kilometres thick Neogene and Quaternary sedimentary cover of the Inner Carpathians and the Pannonian Basin.

The local intracrustal reflections are not well developed along the S04 profile. If they exist, they are sometimes hard to correlate between the shot points. They are mainly confined to the central part of the Bohemian Massif to a distance of 200–300 km along the profile and are visible in the sections from SP 44070, SP 44080, SP 44090 and SP 44100 (Fig. 3—SP 44100, P_1P phase).

As later arrivals, we observe the *P*-wave reflections from the Moho discontinuity (*PmP* phase), usually the strongest phase detected to an overcritical distance of 200–250 km. In the Bohemian Massif, these *PmP* phases form relatively long coda, compared to the strong and short *PmP* pulses observed in the southern part of the profile in the Pannonian area (Fig. 3—SP 44210). In the NW, the Moho reflections are visible as strong reflections with long coda. They are sometimes difficult to correlate consistently for all shot points recording the phase, which may indicate a complex Moho structure as, for example, in the Saxothuringian (Fig. 3—SP 44040).

At long offsets, well-developed overcritical *PmP* phases are observed up to a distance of 200–250 km. However, phase correlations for this group are difficult, and their traveltimes are represented by envelopes of high-amplitude arrivals. For SP 44020, SP 44040 and SP 44050, these phases show apparent velocities of 6.3 km s^{-1}, which indicates relatively low seismic velocities at lower crustal levels under the central part of the Bohemian Massif (Fig. 6).

Only a few record sections showed the Moho refractions (*Pn* phases) clearly enough for reliable correlation. In the Bohemian Massif, they are recorded up to a distance of 250–300 km (e.g. Fig. 3–SP44040, Fig. 4—SP 44020). However, they are pronounced in the Carpathians (Fig. 3—SP 44140) and especially from the shot point SP 44210 in the Pannonian Basin, where they are recorded in the northwest direction up to an offset of 530 km (Fig. 3—SP 44210). The *Pn* phases show an apparent velocity of 8 km s^{-1} on average, especially in the Bohemian Massif. Lower apparent velocities of 7.3 km s^{-1} are detected at the north-western side of the Carpathians and indicate a NW-dipping Moho at a distance of ∼400 km along the profile. In a similar way, the undulations of the *Pn* phase visible in the record section of SP 44210 (Fig. 3—SP 44210, Fig. 9a) reflect the complicated Moho topography and the delay caused by deep sedimentary strata of the Carpathian Foredeep at the transition between the Bohemian Massif and the Carpathians. The crossover distance between the crust and mantle refractions in the Bohemian Massif is 130–140 km, whereas in the SE, in the Pannonian Basin, the crossover distance is 110 km, which indicates a thinner crust of about 24 km in the SE compared to 30–32 km thick crust in the NW.

The upper mantle reflections (P^IP phase) are visible on some record sections especially in the recordings from the Carpathians and the Pannonian Basin (Fig. 9—SP 44210) and document upper mantle reflectors in the central part of the S04 profile. Because some lithospheric phases are not very clear, their determination is more uncertain.

5 SEISMIC MODELLING OF THE CRUST AND THE UPPER MANTLE

To model the structure, we applied forward iterative traveltime fitting using the ray tracing program package *SEIS83* (Červený & Pšenčík 1984) supplemented by an interactive graphical interface *MODEL* (Komminaho 1997) and *ZPLOT* (Zelt 1994). The modelling involved calculating traveltimes and synthetic sections to assess variations in amplitude, traveltime and duration of both the refracted and reflected seismic phases from the crust and uppermost mantle. The traveltimes were used to derive the overall velocity structure; the synthetic sections were used for qualitative comparison of the amplitudes of synthetic and observed seismograms, and helped to constrain the velocity gradients and velocity contrasts at discontinuities. Fig. 4 shows examples of the forward modelling approach for SP 44020 in the Bohemian Massif and SP 44170 in the Carpathians with calculated traveltimes and synthetic sections. This modelling approach results in a final 2-D velocity model presented in Fig. 5.

5.1 Bohemian Massif

In the upper crust of the Bohemian Massif there are the following variations in the *Vp* velocities. Starting in the NW in the Saxothuringian, a near-surface velocity of 6 km s^{-1} at a distance of around 70 km along the profile corresponds to the Palaeozoic metamorphic rocks at the north-western flank of the Krušné Hory/Erzgebirge Mts. (NW of the Eger Rift) followed by lower near-surface velocities of 5.85 km s^{-1} for the granitoids on the other side of this mountain range. Lower velocities of 3.7 km s^{-1} at a distance of 100–150 km along the profile represent Permo-Carboniferous to Tertiary sedimentary successions of local basins down to a depth of 1200 m that are in accordance with the interpretation of Kopecký (1978) or Mlčoch (2001). At a distance of 110 km, these sedimentary successions are penetrated by Tertiary alkaline volcanic rocks of the České Středohoří Mts. with higher near-surface velocities developed at the contact of the Saxothuringian and the Barrandian along the Eger Rift (Reicherter *et al.* 2008). Further to the SE, the velocities of 3.4 km s^{-1} coincide with the embayments of the Bohemian Cretaceous Basin (200 and 280 km along the profile) alternating with the Permo-Carboniferous rocks with velocities of 5.9–6.0 km s^{-1} forming the basement of the Barrandian. The velocity structure reflects the tectonic setting in this area, because the profile runs along the contact of the Barrandian with the northern rim of the Moldanubian, sometimes buried beneath the Mesozoic sedimentary successions of the Bohemian Cretaceous Basin parallel with the southern strand of the Elbe Fault zone (Železné Hory Fault).

Velocities of 6.0 km s^{-1} at a distance of 320 km along the profile represent the metamorphic rocks of the northern rim of the Moldanubian exposed at the surface. They are similar to the velocities modelled by Hrubcová *et al.* (2005) in the central part of the Moldanubian. Lower velocities of 5.7–5.8 km s^{-1} beyond 320 km along the profile correspond to the Palaeozoic metasediments of the Moravo-Silesian unit also observed along the perpendicular CEL10 profile at the eastern edge of the Bohemian Massif (Hrubcová *et al.* 2008).

Deeper parts of the crust in the Bohemian Massif exhibit a very low vertical gradient. This concerns especially the NW end, the Saxothuringian, where the crust was modelled with a *Vp* velocity of 6.1–6.35 km s^{-1} within a depth range of 3–22 km and constrained by overcritical phases of the intracrustal and Moho reflections. An intracrustal reflector in the Saxothuringian was identified at a depth of 12 km; in the Moldanubian, two mid-crustal reflectors were identified at depths of 17 and 22 km.

The velocities in the lower crust can be constrained by well-developed overcritical *PmP* phases usually observed up to 200–250 km offsets. In the central part of the Bohemian Massif, beneath the Barrandian and Moldanubian (SP 44020, SP 44040, SP 44050, and reciprocally SP 44090), the apparent velocities of 6.4 km s^{-1} of these phases indicate low velocities at lower crustal levels (170–230 km along the profile). This is documented for data of SP 44040 in Fig. 6, which shows the response of a 1-D velocity model with such velocities in the lower crust (Fig. 6a) and compares it with the response from a model with higher velocity in the lower crust (Fig. 6b) or a model with decreased velocities in the whole crust (except the uppermost part) (Fig. 6c).

The *PmP* phases are visible as strong reflections with long coda, which are sometimes hard to fit consistently for all shot points, especially in the NW part in the Saxothuringian. To explain such data, several interpretations are, to some extent, possible. First of all, we introduced a higher velocity lower crust similar to that modelled by Hrubcová *et al.* (2005) for the same unit some 70 km further to the SW. This layer with a velocity of about 7 km s^{-1} was located within a depth range of 23–31 km. Compared to Hrubcová *et al.* (2005), where the strongest reflector was from the top of the high-velocity

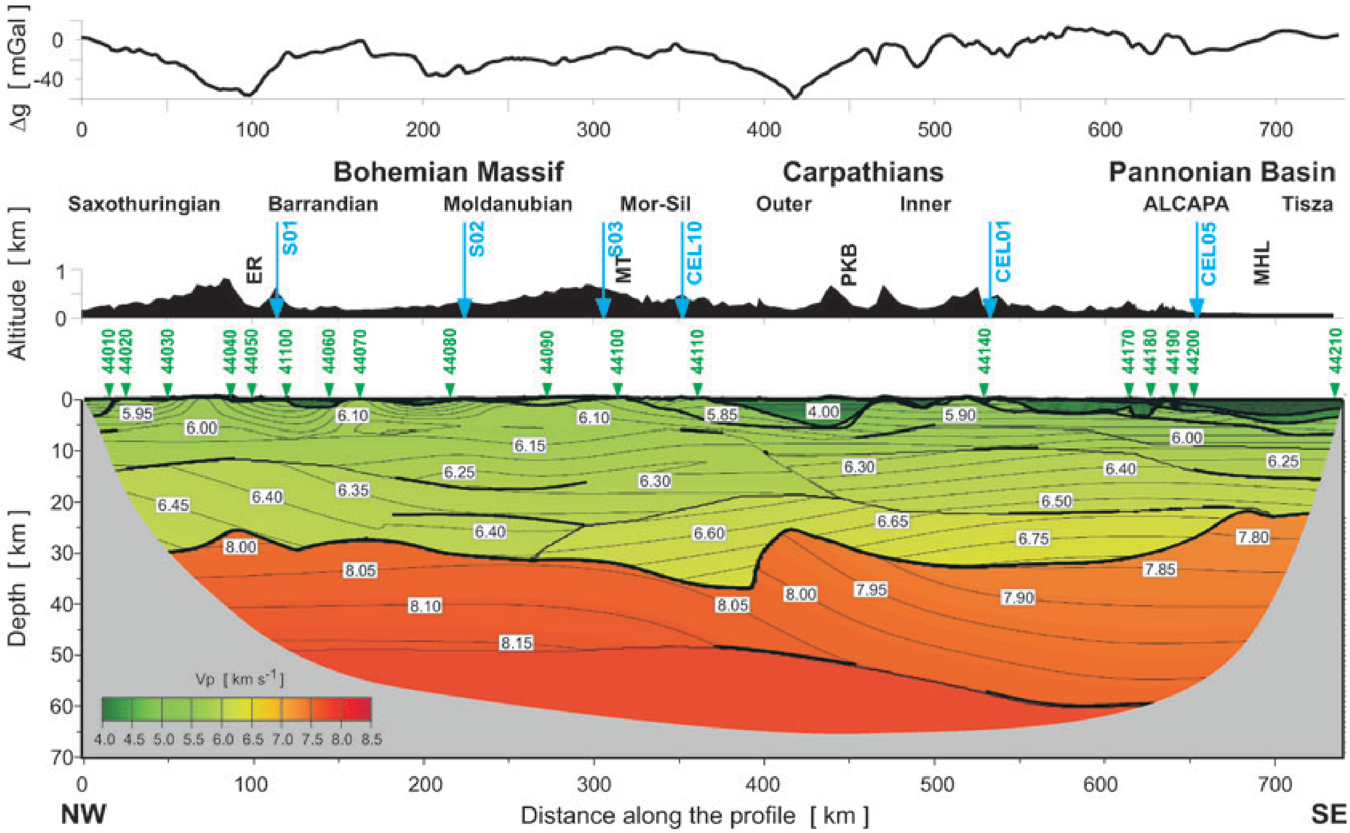

Figure 5. Two-dimensional *P*-wave velocity model for the S04 profile derived from forward ray tracing modelling with *SEIS83* package (Červený & Pšenčík 1984) with elevations and Bouguer anomaly on the top. The grey covers unconstrained parts of the model. Thick lines mark discontinuities constrained by reflections and well-constrained interfaces in the uppermost crust. Thin lines are isovelocity contours spaced at intervals of 0.05 km s^{-1}. Numbered triangles refer to shot points; blue arrows show locations of other refraction and reflection profiles. ER, Eger Rift; MT, Moldanubian Thrust; PKB, Pieniny Klippen Belt; MHL, Mid-Hungarian Line. Vertical exaggeration is 3:1.

lower crust, in this study the Moho is quite dominant. Fig. 7(a) shows the effect of such a structure in the data, where it was possible to fit the traveltimes, but there were difficulties in fitting the synthetic seismograms. This indicated that the velocity contrasts at the top and bottom of the high-velocity lower crust for the S04 data were not accurate. Another way of explaining the data was to model the structure by a double Moho, where some parts of the profile showed reflections from the upper Moho, and some other parts from the lower one. Such an interpretation resulted in a reasonable fit in traveltimes for the reflections, but there was no good fit for the *Pn* phase. The best fit for both the *PmP*, and *Pn* phases is obtained for a simple Moho with some undulations. Such an interpretation corresponds well with the result of the perpendicular profile S01 (Grad *et al.* 2008) and aggress well in traveltimes and synthetics (Fig. 7b).

In the central part of the Bohemian Massif beneath the Barrandian and Moldanubian, the Moho is modelled as a sharp discontinuity at a depth of 28–32 km dipping to the SE. The uppermost mantle velocities are in the range of 8.0–8.05 km s^{-1}.

At the SE end of the Bohemian Massif beneath the Moravo-Silesian, the lower crust shows slightly elevated velocities of 6.6 km s^{-1} compared to those in the Moldanubian with the Moho at a depth of 32–34 km. In the same area, the perpendicular profile CEL10 (Hrubcová *et al.* 2008) showed a gradient zone with velocities of 6.9–7.4 km s^{-1} over a depth range of 26–36 km. Fig. 8 illustrates two possible interpretations of the crust-mantle transition from reciprocal shot points SP 44090 and SP 44140. It compares the *PmP* and *Pn* for a first-order Moho discontinuity with a sharp velocity contrast with phases originating from a high gradient crust–mantle transition zone (as according to Hrubcová *et al.* 2008). The data in this area are not of high quality and some phases are not visible, which allows a wider range of possible solutions. From the calculated traveltimes and the synthetics it is clear that both interpretations would, to some extent, satisfy the data. Although the usual approach is to try to reach an agreement between interpretations on crossing profiles, in our case we decided to keep the first-order Moho discontinuity in the model. Unlike CEL10, the S04 profile is in a more favourable position with respect to the position of the tectonic units. If two interpretations are equal in terms of uncertainty, the model of minimum structure is typically the preferred model. Nevertheless, this is a complicated tectonic area and a gradient zone detected along the refraction profile CEL10 (Hrubcová *et al.* 2008) can still be a matter of debate.

5.2 Transition between the Bohemian Massif and the Carpathians

The upper crustal velocities at the transition between the Bohemian Massif and the Carpathians show pronounced lateral variations compared to the Bohemian Massif. Considerably lower velocities of 3.8–4.2 km s^{-1} were modelled down to a depth of 7 km in a distance range of 370–460 km. They correspond to the Tertiary sediments of the Outer Western Carpathians namely the Carpathian Foredeep

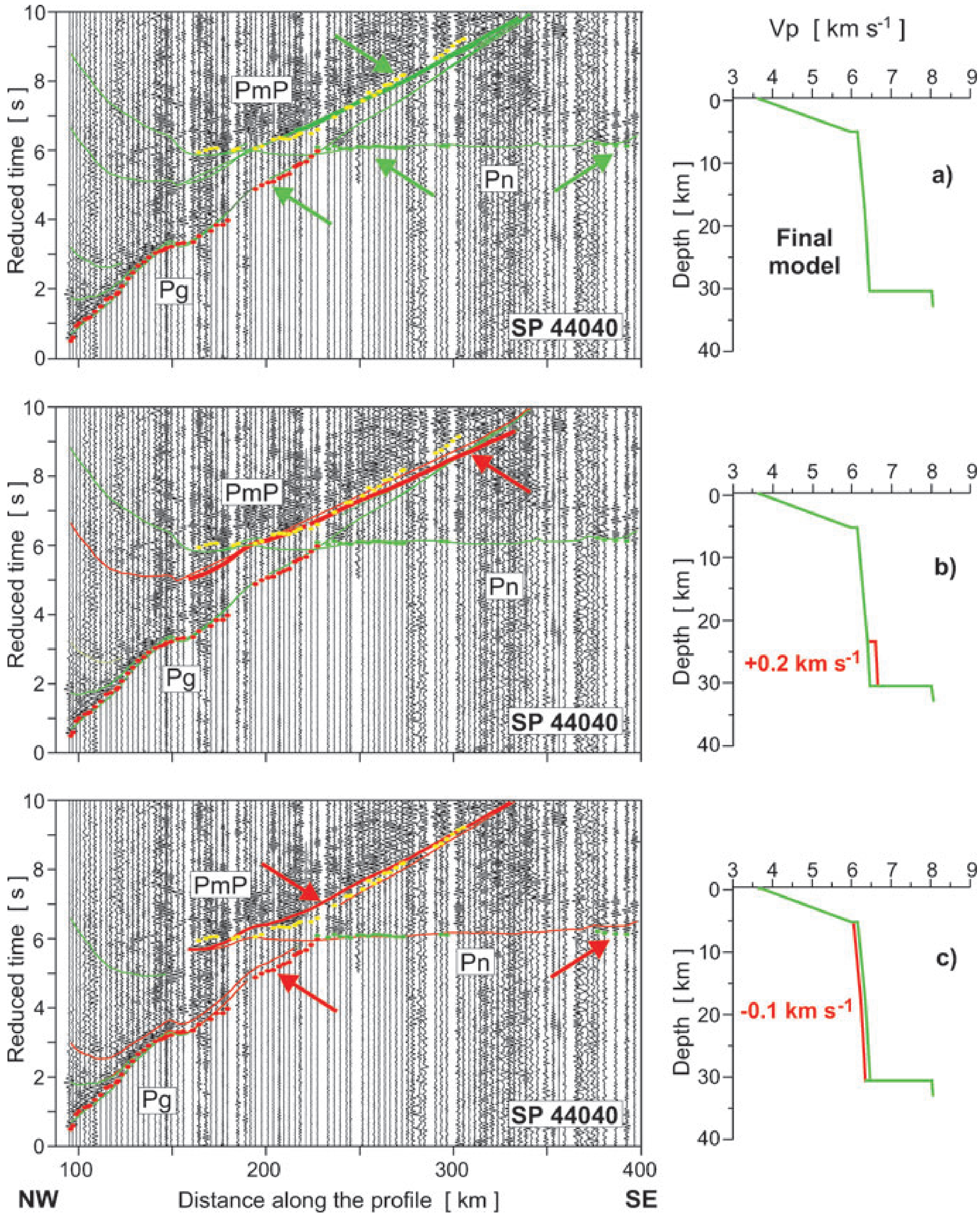

Figure 6. Seismic record sections for SP 44040 with superimposed calculated traveltime curves (left) for different velocity models (right) documenting lower *Vp* velocities in the lower crust interpreted along the S04 profile in the Barrandian and Moldanubian (170–230 km along the profile). (a) Response of a velocity model as in Fig. 5. Note the fit for the lower crustal, overcritical and *Pn* phases (see green arrows). (b) Higher velocities in the lower crust. Note a misfit for the overcritical phases (see red arrow). (c) Decreased velocities in the middle and lower crust. Note a misfit for the *PmP*, overcritical phases, lower crustal and *Pn* phases (see red arrows).

and the Carpathian Flysch. Considering the larger distance between the nearest shot points (SP 44110 at the eastern edge of the Bohemian Massif and SP 44140 in the Carpathians, Fig. 2), this area is not well constrained by the S04 seismic data. Thus, the velocity values modelled along the S04 profile were compared with the ones from the profiles CEL01 and CEL05 (Grad *et al.* 2006; Środa *et al.* 2006) of the CELEBRATION 2000 experiment crossing the same tectonic units. Since the data for SP 44210 in the Pannonian Basin showed a pronounced *Pn* phase visible up to an offset of 500 km, the thickness variation of the Carpathian Flysch and Foredeep sediments with lower velocities was mainly constrained by the *Pn* wave fluctuations from this shot point (Fig. 9). The sedimentary thickness was also constrained by the interpretation of the seismic reflection profile 8HR (Tomek & Hall 1993) and by geological information (e.g. Vozár *et al.* 1999; Golonka & Krobicki 2004). Fig. 9(b) documents the effect of lower velocities of the Carpathian Foredeep

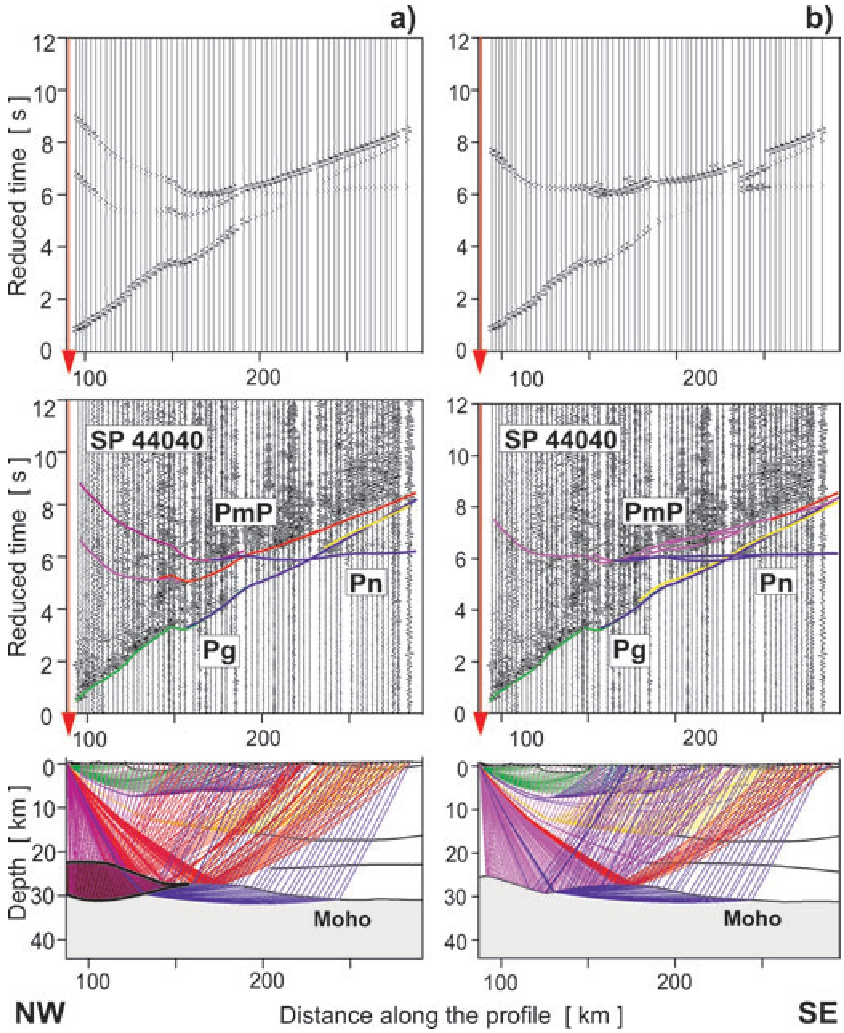

Figure 7. Forward modelling of the lower crust in the Saxothuringian—SP 44040. (a) High-velocity lower crust. (b) Final model as in Fig. 5. For each part of the figure: (top panel) synthetic seismic sections, (middle panel) amplitude normalized record sections with theoretical traveltimes, (bottom panel) model and ray paths. Data have been bandpass filtered from 2 to 15 Hz. Reduction velocity is 8 km s^{-1}. Identification of seismic phases as in Fig. 4. High-velocity lower crust is marked in brown. Note reflections from the top of the lower crust visible in the synthetic seismic section and not corresponding with the data in (a) compared to a good fit of data with the synthetic section in (b).

and Flysch and shows a good fit of the traveltimes with the data for the model where lower velocities of the Carpathian Foredeep and Flysch were introduced (*Pn* phase—violet line) compared to the effect of missing sedimentary successions where traveltimes come too early to fit the data (marked by blue). The final results also correspond with the interpretation along the reflection profile 8HR (Tomek & Hall 1993; Hubatka & Švancara 2002). Very low velocities of 2.2 km s^{-1} to a depth of 0.5 km at the distance of 425 km reflect the Neogene to Quaternary sediments of the Vienna Basin margin.

The crust–mantle transition at the contact of the Bohemian Massif and the Carpathians shows strong lateral variations and the Moho within a depth range of 26–37 km. The Moho in this area is not constrained by reflections but by refractions from the upper mantle. The apparent velocity of 7.3 km s^{-1} for the *Pn* phase from SP 44140 in the Carpathians indicates a NW-dipping Moho at a distance of 390–415 km along the profile (Fig. 8a—SP 44140). A similar effect is visible in the data of SP 44210 where the apparent velocity of 7.3 km s^{-1} at a distance of 315–380 km along the profile for the *Pn* phase reflects the Moho dip to the NW in the same area. It is followed by an apparent velocity of 8.5 km s^{-1} at a distance of 210–290 km along the profile, which corresponds to the opposite, SE dip of the Moho at 290–370 km. To confirm the interpretation, Fig. 9 shows the effect of the sharply dipping Moho at the contact of the Bohemian Massif with the Carpathians in contrast to the response from a model with a flat Moho. In the case of the Moho uplift and dip, the fit for *Pn* was achieved for picks at a distance of 325–400 km along the profile and also for strong second arrivals at a distance of 290–310 km (Fig. 9a), which is missing in the case of a flat Moho (Fig. 9b, marked by red arrows).

5.3 Western Carpathians and the Pannonian Basin

Leaving the Carpathian Foredeep and the Flysch Belt, the profile continues across the Inner Carpathians. Velocities of 5.8–5.9 km s^{-1} further to the SE represent the core mountains composed of the pre-Alpine basement and its Mesozoic sedimentary cover (McCann 2008b). At a distance of 490 and 530 km they alternate with lower velocities representing the sediments of the Pannonian Basin. Andesitic and rhyolitic rocks of the Tertiary volcanic edifices

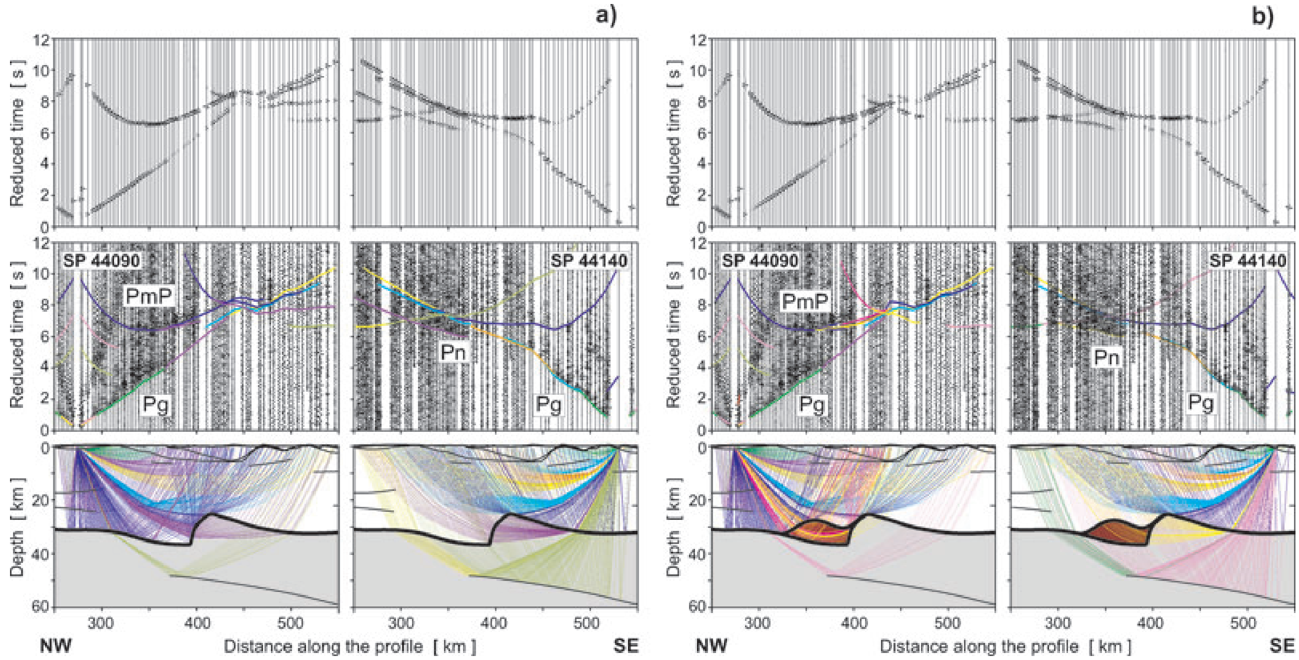

Figure 8. Forward modelling for reciprocal shot points SP 44090 and SP 44140 illustrating the character of the crust–mantle transition in the Moravo-Silesian. (a) Velocity contrast at the Moho as in Fig. 5. (b) High gradient crust–mantle transition zone according to the CEL10 interpretation (Hrubcová *et al.* 2008). For each part of the figure: (top panel) synthetic seismic sections, (middle panel) amplitude normalized record sections with theoretical traveltimes, (bottom panel) model and ray paths. Data have been bandpass filtered from 2 to 15 Hz. Reduction velocity is 8 km s^{-1}. High-velocity lower crust is marked in brown.

are reached at 520–545 km along the profile followed by volcano-sedimentary complexes to a distance of 560 km. Elevated velocities at a distance of 610–650 km along the profile represent the western slopes of a Tertiary volcanic complex in northern Hungary. Low velocities of 2.2–4.2 km s^{-1} down to a depth of 4.5 km from a distance of 650 km reflect the Neogene and Quaternary sediments of the Pannonian Basin in Hungary.

Two isolated reflectors were detected at the depths of 10 and 20 km in the middle crust of the central part of the Carpathians. The lower crust displays velocities of 6.8 km s^{-1} and the Moho is modelled at the depth of 32–34 km.

Beneath the Pannonian Basin, the *PmP* phase is the most pronounced in terms of high amplitude and short coda. The Moho is interpreted as a first-order discontinuity at a depth of 23 km with a sharp velocity increase from 6.5 to 7.8–7.9 km s^{-1}. This is in agreement with other geophysical interpretations in this area (Posgay *et al.* 1981; Bielik *et al.* 2004; Grad *et al.* 2006; Środa *et al.* 2006).

Two upper mantle reflectors at the distances of 370–460 and 530–630 km along the profile are visible at the depth of 50–60 km (Fig. 3—SP 44100, SP 44140 and SP 44210). They dip from the eastern edge of the Bohemian Massif to the central part of the Carpathians. Since some lithospheric phases constraining them are not very clear, their determination is more uncertain. Velocities beneath these reflectors (8.3 km s^{-1}) have an even higher uncertainty because there is no reciprocity and they are only constrained by the data of SP 44210.

6 ANALYSIS OF ACCURACY, RESOLUTION AND UNCERTAINTIES

Modelling errors result from a combination of several factors: data timing errors, misidentification of seismic phases, traveltime picking, inaccuracy of modelling (misfit between data and modelled traveltimes) and 2-D geometry of the experiment, not accounting for 3-D effects or anisotropy. Some errors are subjective, introduced by the interpreter during phase correlation, and cannot be quantified. Their magnitude decreases with increasing quality and quantity of data. Due to the subjective errors, it is not possible to produce a full and systematic error analysis. In this study, we attempt to evaluate the errors resulting from picking accuracy and from the misfit between the model and the data. Also, in the process of modelling, the limitations of the ray theory must be kept in mind. In addition, two-dimensional modelling does not take into account out-of-plane refracted and reflected arrivals, which must have occurred particularly in such a structurally complex area and at the contacts of several units.

In the interpreted data set, the major phases were correlated with considerable confidence, increased by comparisons of phases picked independently by different interpreters and with the help of reciprocity checking. The following criteria were used to decide whether a given phase can be used for constraining the model: the signal-to-noise ratio is high enough to isolate the phase from the noise as a series of pulses on neighbouring seismograms, the continuity of the group of pulses over some distance interval and the phase's apparent velocity, which should roughly fit the range of plausible crust/mantle velocities. The important test for the credibility of the phases, which significantly reduces the non-uniqueness of the phase identification, was the reciprocity checking: a phase that could be picked consistently (i.e. with the same traveltime at the reciprocal shot location) for several shot points was assumed to represent a major structure extending over a considerable part of the model and was included in the modelling. The phases that did not pass the reciprocity test were not used for modelling. This was mostly the case of short groups of second arrivals with average amplitude, representing the most likely reflections (possibly side-reflections) or diffractions from local, relatively

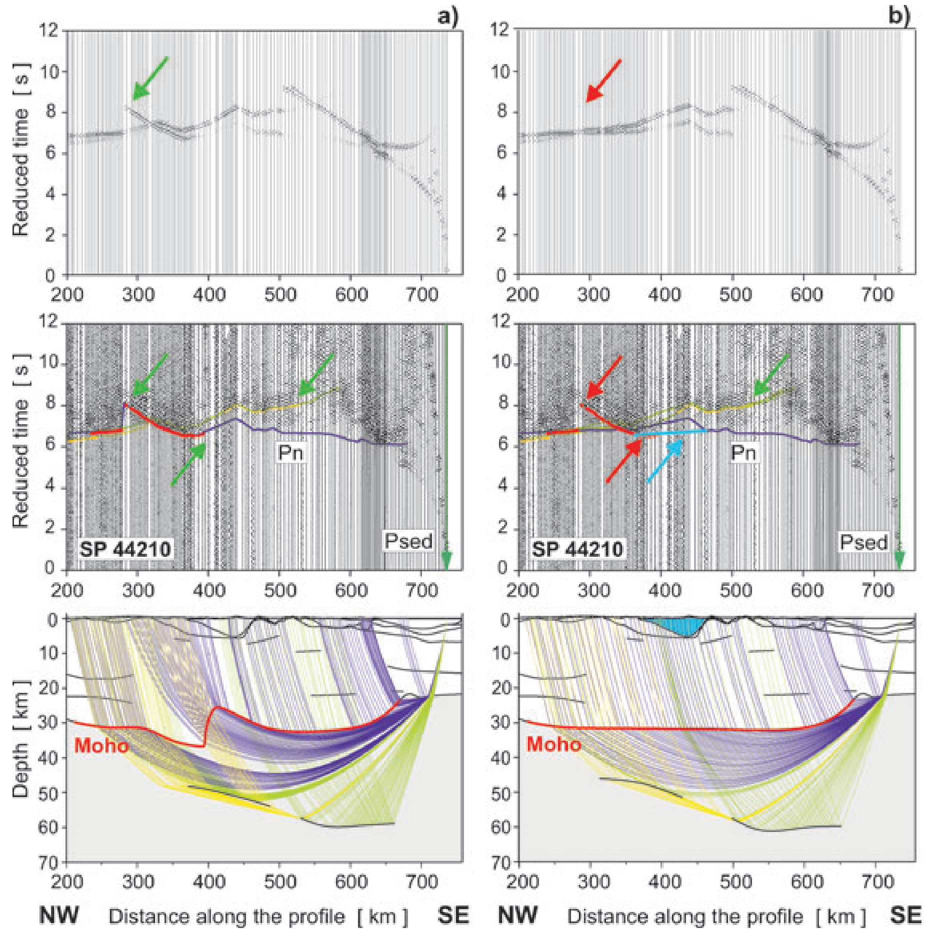

Figure 9. Forward modelling for SP 44210 documenting the Moho at the transition between the Bohemian Massif and the Carpathians. (a) dipping Moho, (b) flat Moho. For each part of the figure: (top panel) synthetic seismic sections, (middle panel) amplitude normalized record sections with theoretical traveltimes, (bottom panel) model and ray paths. Data have been bandpass filtered from 2 to 15 Hz. Reduction velocity is 8 km s^{-1}. *Pn*, refraction from the uppermost mantle (violet line). Green arrows mark the Moho effect response. Note good fit for *Pn* and strong second arrivals with picks (marked in red in the middle panel) in the case of the dipping Moho (a) compared to a missing response (marked by red arrows) for picks (marked in red in the middle panel) in the case of a flat Moho (b). Note in case (b) good fit of traveltimes with the data where lower velocities in the Carpathian Flysch were introduced compared to the effect of the model without these velocities that come too early to fit the data (marked by blue line and blue arrow).

small-scale anomalies or discontinuities. The most credible phases were usually the *Pg* and *Pn* as the first arrivals, characterized by a high signal-to noise ratio. However, in some areas they were not visible (mainly the *Pn* phase). As for the second arrivals, the *PmP* phase was the easiest to correlate due to its high amplitude. However, for several shot points it could not be reliably correlated reciprocally due to a low signal-to-noise ratio and scatter of its onsets. The mantle phases (*Pn* and P^lP) from SP 44210 were used for modelling, although they could not be confirmed by the reciprocity test—their very high amplitude due to a large charge provide the excellent data to enable confident modelling of the abrupt changes in the Moho topography and thickness of the Carpathians sedimentary foredeep.

The picking accuracy was usually about ±0.05–0.1 s for the *Pg* phases (smaller especially for the near-offset arrivals) and about ±0.1–0.2 s for the reflected phases (*PmP*, midcrustal reflections) and the *Pn*. The calculated traveltimes fit the observed ones with an accuracy of ±0.2 s on average for both refracted and reflected phases. In the ray tracing modelling, we analyse traveltime curves rather than single arrivals and in such cases, typical velocity errors were about 0.1 km s^{-1} and errors in the boundary depth determinations were of the order of 1 km. However, in complicated or poorly constrained parts of the model, they might increase up to 0.2 km s^{-1} and 2 km, respectively. In addition, synthetic seismograms generally showed good qualitative agreement with the relative amplitudes of the observed refracted and reflected phases. Fig. 10 presents traveltime residuals, as well as diagrams of ray coverage and observed reflections along modelled seismic discontinuities. The average of the residuals is close to zero, which means that there is no systematic deviation of the model parameters with respect to the data.

7 GRAVITY

Following the derivation of the seismic velocity structure, we used gravity modelling to test the seismic model and to obtain additional geophysical constraints on the crustal structure and composition. In a first approximation, we converted the *P*-wave velocity model (Fig. 5) into densities using the velocity–density relation of Christensen & Mooney (1995) for crustal and upper mantle velocities of 6–8 km s^{-1} and Ludwig *et al.* (1971) for sedimentary velocities. This resulted in an initial density model. Using the 2-D modelling software GRDGRAVITY developed by *I. Trinks* (internet freeware code), we compared the gravity effect of this initial density model with the Bouguer anomaly values (Bielik *et al.* 2006)

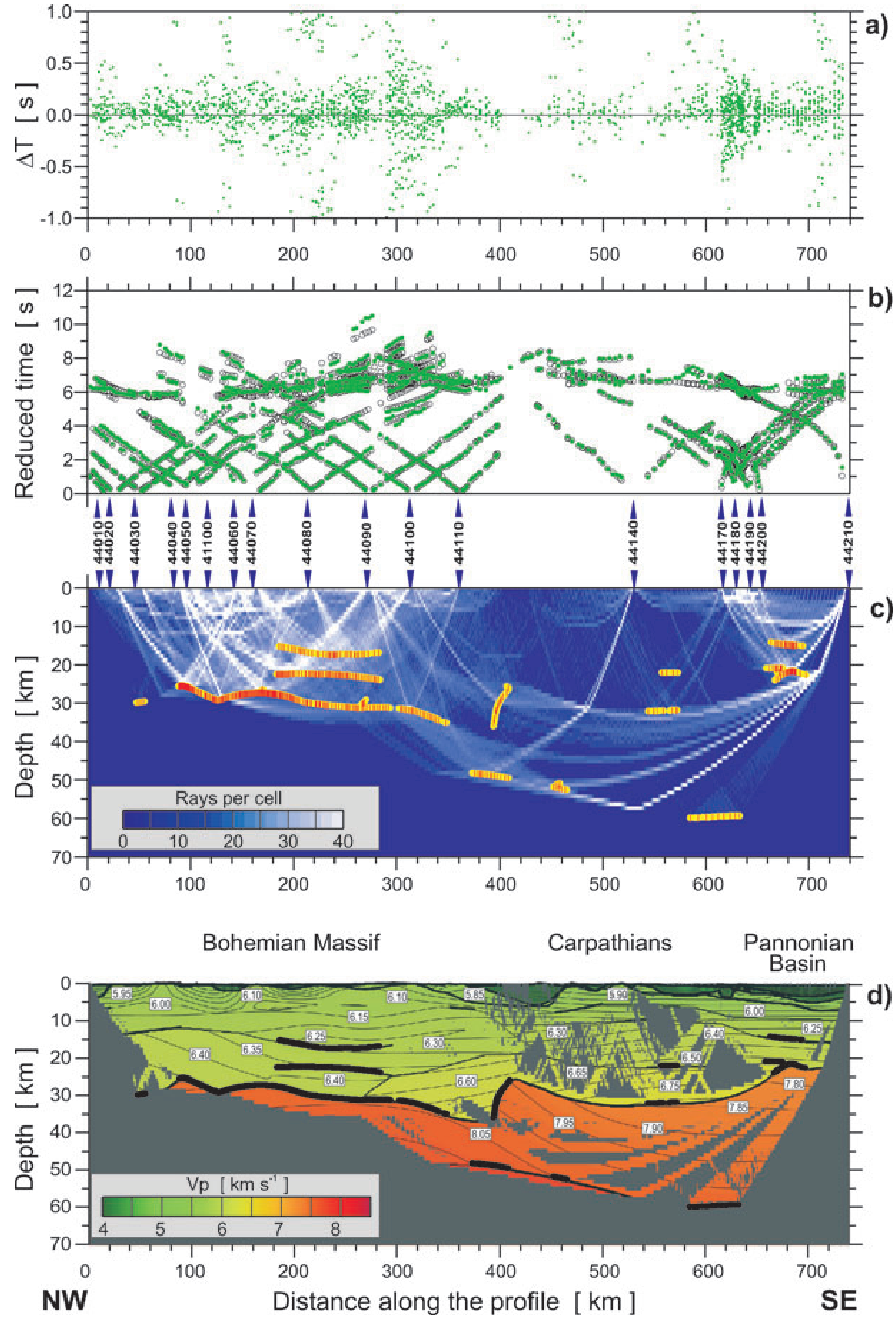

Figure 10. *P*-wave velocity model for the S04 profile (as in Fig. 5) with superimposed rays. (a) Traveltime residuals. (b) Misfit between the observed (green dots) and calculated (black circles) traveltimes. (c) Ray coverage and observed reflecting elements along modelled seismic discontinuities. (d) Model with rays.

along the profile. We then modified the densities in the model, where needed, by the trial-and-error approach to obtain a better fit to the Bouguer anomaly values. The aim was not to obtain a detailed density model but to test the reasonability of the seismic velocities.

Fig. 11 shows the observed Bouguer anomaly together with the gravity responses of the initial and final density models. From the response of the initial model, we can see that the most prominent discrepancies (about 50 mGal) occur in the Saxothuringian in a distance range of 60–120 km along the profile and at the contact of the Bohemian Massif with the Carpathian Flysch Belt in a distance range of 380–440 km. They are in places where the negative Bouguer anomaly reaches a value of −60 mGal.

The gravity minimum in the Saxothuringian coincides with the location of low-density granites in the eastern part of the Krušné Hory/Erzbegirge Mts. (NW of the Eger Rift). There the differences between the granitoids and orthogneisses and neighbouring

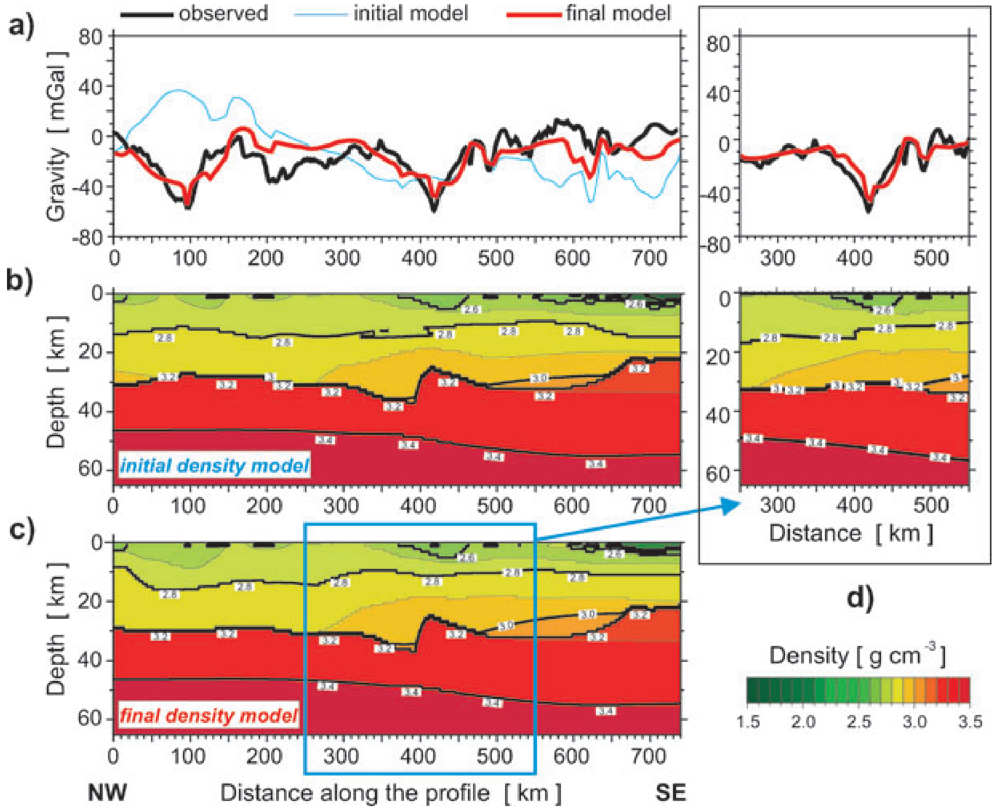

Figure 11. Gravity modelling. (a) Bouguer anomaly (black line), calculated gravity effect from initial density model (blue line) and from final density model (red line). (b) Initial gravity model converted from seismic velocity model in Fig. 5. (c) Final gravity model. (d) Insert showing the gravity effect of a flat Moho at the contact of the Bohemian Massif with the Carpathians.

metamorphic rocks are more pronounced in densities (about 0.1 g cm^{-3}) than in seismic velocities. A similar effect was also encountered along the CEL09 profile (Hrubcová *et al.* 2005) in the Karlovy Vary area, where such a discrepancy was due to a larger density difference between the Karlovy Vary granites and the surrounding rocks than estimated from the seismic velocity–density relationship. To get the fit with the observed Bouguer data, the Saxothuringian anomaly was modelled by lower densities of about 2.60–2.65 g cm^{-3} to a depth of 8–12 km, which is consistent with the results of Behr *et al.* (1994) along the MVE-90 profile. It is also in agreement with the interpretation of Blecha *et al.* (2009) who modelled the same densities and depths for the gravity minimum of the Karlovy Vary pluton further to the SW.

The other pronounced gravity low in the Carpathians is attributed to low-density foredeep and flysch sediments. To achieve the fit in this area it was necessary to introduce lower densities of 2.45 g cm^{-3} than those, which ensued from the velocity-to-density conversion. The discrepancy between the seismic and gravity models can be seen in several factors. Due to the insufficient amount of seismic refraction data as well as seismic attenuation in porous sedimentary rocks, the resolution of the seismic model in the Carpathian Flysch Belt is lower than in some other parts of the profile. Another contributing factor might be the 3-D influence of the Carpathian low anomaly, not taken into account in the 2-D velocity modelling. However, the aim was to test the 2-D velocity results, therefore, we confined the gravity modelling to two dimensions. The local gravity minimum at a distance of 425 km was explained by densities of 2.2 g cm^{-3} and coincides with the light Neogene to Quaternary sedimentary rocks of the Vienna basin margins.

Other smaller corrections (positive and negative) were made in some other parts of the profile mainly in the upper crust. They explain the anomalies usually caused by numerous granitic, mafic and volcanic rocks occurring along the profile or in its close vicinity and producing gravity effects not accounted for by the velocity modelling. The local gravity lows along the profile were explained by small sedimentary Neogene to Quaternary basins not detected by the refraction seismic data as, e.g. the very pronounced anomaly at a distance of 95 km representing the Most sedimentary Basin at the eastern margin of the Krušné Hory/Erzgebirge Mts.

During gravity modelling, different seismic models of the lower crust and Moho were also tested for their gravity effects. In such a way, the high-velocity lower crust under the Saxothuringian revealed a misfit in the gravity data, which was another indication not to promote such a structure in the model. Under the eastern side of the Bohemian Massif, the lower crust can be modelled by slightly higher densities than those which ensue from seismic velocities but not as high as to correspond to the high-velocity zone along the CEL10 profile in the Moravo-Silesian. At the transition between the Bohemian Massif and the Carpathians, the gravity modelling does not constrain our seismic interpretations, because there is neither evidence for the Moho dip nor evidence for a flat Moho and both results show a similar gravity response (Fig. 11). However, we chose the model with the dipping Moho, because it fits the seismic data much better with a very good fit for *Pn* and later arrivals, and because the seismic interpretation excludes a flat Moho (Fig. 9—SP 44210). The Pannonian gravity high results from the Moho rising significantly to about 25–30 km and corresponds with seismic interpretations as well as the results of Bielik *et al.* (2004).

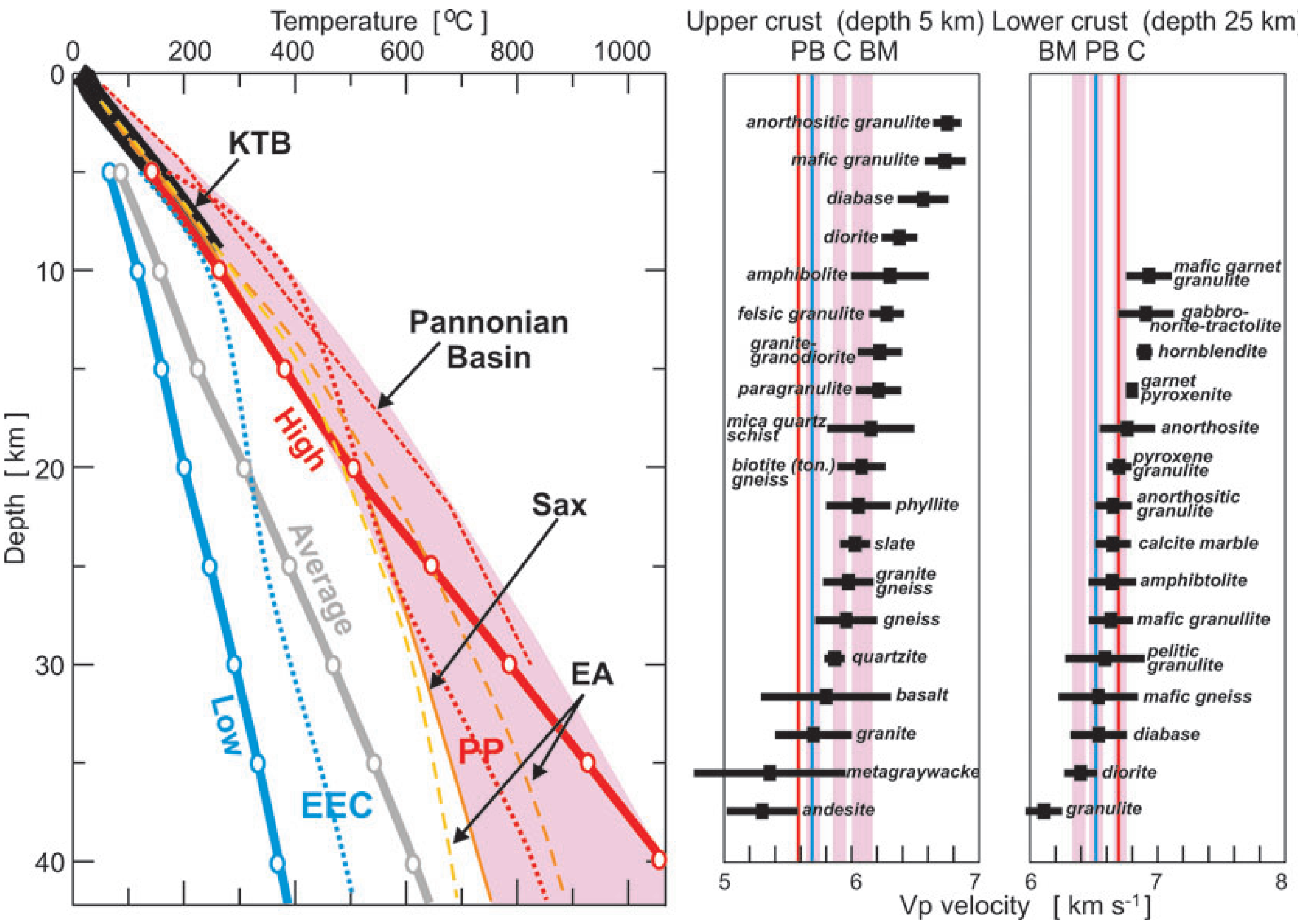

Figure 12. (Left panel) Geothermal gradients. (Right panel) Comparison of the *Vp* velocities observed along the S04 profile with laboratory data. (Left panel) As a reference, temperature–depth curves are shown for low, average and high heat flow regimes (thick blue, grey and red lines with circles) according to Christensen & Mooney (1995). For comparison, temperature–depth curves are shown for the area of the S04 profile, including the Saxothuringian (Sax) (Čermák 1995), Palaeozoic Platform (PP) in southwest Poland (Majorowicz 1976) and Pannonian Basin (PB) (Posgay *et al.* 2001), as well as for neighbouring areas, including 'hot' Eastern Alps (EA) (Vosteen *et al.* 2003), and 'cold' East European Craton (EEC) in northeast Poland (Majorowicz 1976). Thick black line extending to about 10 km shows measured temperature in KTB deep borehole (Emmermann & Lauterjung 1997). Shaded pink area represents 'hot' crust for the area close to the S04 profile. (Right panel) Laboratory data for various rock assemblages (Christensen 1974; Christensen & Mooney 1995; Mueller 1995; Weiss *et al.* 1999; Grégoire *et al.* 2001) are shown for the high temperature model in the crust at 5 and 25 km depth and plotted as black boxes with black lines representing their error estimates. Anisotropy is not considered. Shaded vertical pink bars represent modelled *Vp* values beneath the S04 profile for the upper crust—6.0–6.15 km s^{-1} for the Bohemian Massif (BM), 5.9 km s^{-1} for the Carpathians (C) and 5.7 km s^{-1} for the Pannonian Basin (PB), and for the lower crust–6.4 km s^{-1} for the Bohemian Massif, 6.7 km s^{-1} for the Carpathians and 6.5 km s^{-1} for the Pannonian Basin. The bars are shown with estimated uncertainty of the velocity values of $\pm$0.05 km s^{-1}. Red lines represent average velocities for extended crust (5.59 $\pm$ 0.88 km s^{-1} for 5 km depth, 6.69 $\pm$ 0.30 km s^{-1} for 25 km depth), while blue lines represent velocities for orogens (5.69 $\pm$ 0.67 km s^{-1} for 5 km depth, 6.53 $\pm$ 0.39 km s^{-1} for 25 km depth) (Christensen & Mooney 1995).

8 DISCUSSION OF THE GEOLOGICAL AND TECTONIC IMPLICATIONS

In the following discussion, we propose a general tectonic/geological interpretation for the velocity models along the S04 profile. We discuss these units and their contacts based on the *Pg* velocity distribution, character of the lower crust and Moho topography, surface geology and results from other profiles, especially CEL09, CEL10, S01, S02, S03, 8HR and MT-15. Above, we have shown the additional constraint on the crustal structure given by the gravity modelling. We are aware that, due to the ambiguity of modelling, there can be several possible interpretations, but because of all the mentioned reasons we believe that our proposed interpretation gives one of the most plausible solutions. In our interpretation, we concentrate on velocity variations along the profile. Azimuthal anisotropic studies are a matter of other investigations (e.g. Růžek *et al.* 2003; Vavryčuk *et al.* 2004).

8.1 Crustal lithologies

The interpretation of crustal lithologies along the S04 profile is based on the *P*-wave velocities obtained by 2-D ray tracing modelling. The most plausible lithologies along the profile are inferred from the modelled *Vp* values and compared with global (Christensen & Mooney 1995; Weiss *et al.* 1999) and regional (Christensen 1974; Mueller 1995; Grégoire *et al.* 2001) laboratory data for various crustal rock assemblages. The left part of Fig. 12 shows the temperature–depth curves for the low, average and high heat flow thermal regimes according to Christensen

& Mooney (1995). In the crust of the S04 profile, the published temperature–depth curves for the Saxothuringian (Čermák 1995), the Palaeozoic Platform in southwest Poland (Majorowicz 1976), the Eastern Alps (Vosteen *et al.* 2003), and the Pannonian Basin (Posgay *et al.* 2001) lie close to the high heat-flow curve. This curve also fits the temperatures measured directly in the KTB borehole in the Saxothuringian to a depth of about 10 km (Emmermann & Lauterjung 1997). On the other hand, much lower temperatures are observed for the 'cold' East European Craton in northeast Poland (Majorowicz 1976).

The right part of Fig. 12 shows lithological candidates for a high-temperature regime in the upper (5 km depth) and lower (25 km depth) crust according to Christensen & Mooney (1995) and Mueller (1995), where anisotropy has not been taken into account. The original data of Christensen (1974), Weiss *et al.* (1999) and Grégoire *et al.* (2001) were corrected downward by 0.3 km s^{-1} to adjust for *in situ* temperature conditions. Various rock assemblages are plotted as black boxes with their error estimates. Shaded vertical pink bars represent modelled *Vp* values beneath the S04 profile: upper crust—from 6.0 to 6.15 km s^{-1} for the Bohemian Massif (BM), 5.9 km s^{-1} for the Carpathians (C) and 5.7 km s^{-1} for the Pannonian Basin (PB); lower crust—6.4 km s^{-1} for the Bohemian Massif, 6.7 km s^{-1} for the Carpathians and 6.5 km s^{-1} for the Pannonian Basin. For comparison, the average values according to Christensen & Mooney (1995) are shown, where red lines represent velocities for the extended crust (5.59 ± 0.88 km s^{-1} for 5 km depth, 6.69 ± 0.30 km s^{-1} for 25 km depth), and blue lines represent velocities for orogens (5.69 ± 0.67 km s^{-1} for 5 km depth, 6.53 ± 0.39 km s^{-1} for 25 km depth). The velocities in the Pannonian Basin seem to fit the values for orogens at both 5 and 25 km depths, while those in the Carpathians seem to correspond more to the values for the extended crust. McCann (2008b) points out that, despite being a part of the Alpine-Carpathian Orogen, the Western Carpathians are different from other orogens such as the Alps. The Carpathians underwent a diverse tectonic evolution, which lacks an orogenic root typical for the Eastern Alps (Brückl *et al.* 2007). Our result can, to some extent, reflect this diversity. Also, it should be noted that the values of Christensen & Mooney (1995) represent averages of a broad range of velocities for given types of crust.

The upper crystalline crust of the Bohemian Massif (at a depth of 5 km) is characterized by velocities from 6.0 to 6.3 km s^{-1}, which are typical of basement rocks of Cadomian age in the Barrandian unit and the mid-Palaeozoic Variscan granitoids and gneisses in the Moldanubian unit exposed in some places at the surface. The Cadomian basement is also present in the Saxothuringian zone consisting of volcano–sedimentary complexes overlain by Palaeozoic strata. The lower crust of the Bohemian Massif (at the depths from 15 to 30 km) displays velocities of 6.4–6.5 km s^{-1}. These relatively low values reflect a continuing predominance of felsic lithologies towards the base of the crust. Similar velocities were obtained along the MVE-90 reflection profile, where they were interpreted as being related to gneisses with a varying content of metabasites (or mafic gneisses) (see Behr *et al.* 1994). Pelitic granulites can represent other candidates for the major rock components in the lower crust. Restites from the huge granite bodies of the upper crust are present in the middle-to-lower crust of the Saxothuringian zone and would be in agreement with the modelled velocities. There seems to be no major imprint of the Cenozoic magmatism in the overall velocity structure in the area of the Eger Rift (České Středohoří).

Lower upper crustal velocities of 4.2–4.3 km s^{-1} (depth of 5 km) at the transition between the Bohemian Massif and the Carpathians reflect the sedimentary infill of the Carpathian Foredeep as the eastward prolongation of the East Alpine Molasse basin and forming a characteristic clastic wedge thinning towards the foreland. It is followed by rocks of the Carpathian Flysch Belt, composed exclusively of Jurassic to Miocene sediments such as schists, sandstones and their conglomerates that were scraped off the subducted basement of the Carpathian embayment. In the Carpathians, upper crustal velocities of 5.9 km s^{-1} (depth of 5 km) represent various pre-Tertiary units and the unconformable Cenozoic volcanic complexes (rhyolites to dacites) alternating with lower velocities of the sedimentary complexes at the surface (McCann 2008b).

Lower crustal *P*-wave velocities of 6.6–6.7 km s^{-1} under the SE rim of the Bohemian Massif (Moldanubian/Moravo-Silesian) are slightly higher than those further to the northwest (6.4–6.5 km s^{-1}), indicating slightly more mafic composition and potentially different tectonic origin. The lower crust under the Carpathians is characterized by *P*-wave velocities from 6.7 to 6.8 km s^{-1}, indicating a more mafic composition than that in the Bohemian Massif (amphibolites, mafic granulites) although the difference is not very high. Lower crustal velocities of 6.5 km s^{-1} are typical for the Pannonian Basin. There, the lower crust might consist of various types of granulites as is evident from the xenoliths, which were brought to the surface by the Cenozoic volcanism (e.g. Kempton *et al.* 1997; Embey-Isztin *et al.* 2003). However, their compositions indicate a more mafic lithology than shown by the S04 *P*-wave velocities in this area.

Low velocities in the lower crust under the Bohemian Massif (the Saxothuringian, Teplá-Barrandian and Moldanubian zones) are in agreement with observations all over the Variscan orogenic belt up to the Central Iberian System (Villaseca *et al.* 1999) and maybe even across the Atlantic to the Southern Appalachians (Taylor & Toksöz 1982). Xenolith studies (e.g. Downes 1993; Wedepohl 1995; Villaseca *et al.* 1999) indicate that the lower crust of the Variscan internides may actually be dominated by felsic rock types (felsic/metapelitic granulites, charnockites, restites).

The Moravo-Silesian Zone is more or less equivalent to the Mesozoic Bohemian-Tethyan continental margin. This zone is characterized in its eastern part by strong total magnetic anomalies (Lenhardt *et al.* 2007), which are not too different from anomalies along present-day continental margins. Slightly increased velocities in comparison to the central Bohemian Massif may indicate that the lower crust of the former passive margin was overprinted/modified during the Mesozoic rifting.

8.2 Comparison with other refraction lines

One way to decrease the ambiguity of the interpretation was to compare model velocities with other results in the area, especially when there are models for other refraction profiles as is the case of the S04 line (Fig. 2). Fig. 13 shows the velocity–depth profiles extracted from crossing models (in blue) and compares them to those for S04 (in red) at the intersections. In general, *P*-wave velocities from the S04 model agree with those from the other models. A discrepancy is visible in the Moravo-Silesian where the S04 profile images the Moho discontinuity with a velocity increase from 6.7 to 8.0 km s^{-1} at a depth of 33 km compared to the broad high gradient zone with no sharp discontinuities over a depth range from 26 to 36 km (velocities of 6.9–7.4 km s^{-1}) modelled along the CEL10 profile. In the Carpathians, the Moho depth modelled along the S04 profile is slightly deeper (32 and 28 km) than in the case of the crossing profiles CEL01 and CEL05 (30 and 25 km). A final tectonic sketch based on the geophysical modelling along the S04 profile is shown in Fig. 14.

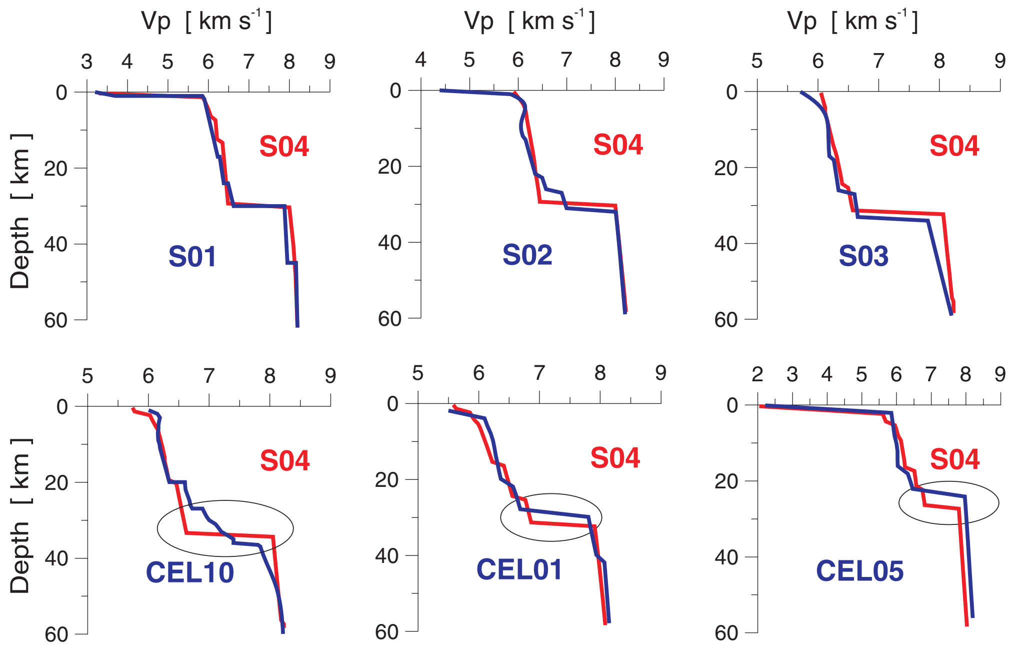

Figure 13. Velocity–depth models from the S04 profile (red lines) with velocity–depth models at intersections with the S01, S02, S03, CEL10, CEL01 and CEL05 profiles (blue lines) (Grad *et al.* 2006, 2008; Majdański *et al.* 2006; Środa *et al.* 2006; Hrubcová *et al.* 2008). Ellipses mark the parts of the models discussed in detail in the text.

8.3 Tectonic development of the Bohemian Massif

The Saxothuringian displays a near-surface velocity of 6 km s^{-1}, representing the Palaeozoic metamorphic rocks at the north-western flank of the Krušné Hory/Erzgebirge Mts. (NW of the Eger Rift). Lower velocities of 5.85 km s^{-1} in the upper crust at the contact of the Saxothuringian and Barrandian correspond to the gravity minimum of the low-density granites. The contrast between the granites and neighbouring rocks is more pronounced in densities than in seismic velocities and according to the gravity modelling the granites are seated 8–12 km deeper than anticipated from the seismic interpretation. Such a result is in agreement with the interpretation of Blecha *et al.* (2009) who modelled the same densities and depths for the gravity minimum of the Karlovy Vary Pluton further to the SW.

The structure of the lower crust and the Moho under the Saxothuringian is difficult to determine unequivocally with the available seismic information. The data in this area allow several possible interpretations, some of them more favourable than others, although none of them fits all the seismic data. We tested a higher velocity lower crust similar to that modelled by Hrubcová *et al.* (2005) where its extent indicated the continuation of the Saxothuringian unit at depth. However, compared to Hrubcová *et al.* (2005) where the strongest reflector was from the top of the high-velocity lower crust, in our data the Moho was quite pronounced. A similar way of explaining the data was to model the structure by a double Moho where some parts showed reflections from the upper Moho, and some from the lower one. This interpretation resulted in a reasonable fit in traveltimes for the reflections, but not for the upper mantle refraction. Also, the high-velocity lower crust revealed a misfit in the gravity data, which was another indication not to promote such a structure in the model. In our interpretation as in Fig. 5, we tend to model the Moho as a sharp velocity contrast with some undulations which might indicate some young tectonic processes at the Moho level. Such an interpretation corresponds well with the result of the perpendicular profile S01 (Grad *et al.* 2008) (Fig. 13) and agrees well in terms of traveltimes and synthetics.

The upper crust at the northern rim of the Moldanubian displays velocities of 6.0 km s^{-1}, representing the metamorphic rocks exposed at the surface. Their seismic velocities are similar to those modelled by Hrubcová *et al.* (2005) under the central part of the Moldanubian. Gravity highs in this area are caused by metamorphosed Proterozoic and lower Palaeozoic rocks containing abundant mafic bodies (McCann 2008a). The profile intersects the area parallel to the contact of the Moldanubian and Barrandian, which is partly buried beneath the Bohemian Cretaceous Basin. The margins of this basin are seen with slightly lower velocities reflecting the Mesozoic sedimentary sequences. The lower crust in the central part of the Bohemian Massif under the Barrandian and Moldanubian shows velocities of 6.4 km s^{-1} constrained by well-developed overcritical crustal phases usually observed up to offsets of 200–250 km. The Moho is modelled as a first-order discontinuity at a depth of 28–34 km, slightly dipping to the SE.

At the SE end of the Bohemian Massif under the Moravo-Silesian, the lower crust along the S04 profile displays slightly elevated velocities of 6.6 km s^{-1} compared to those in the Moldanubian with the Moho at a depth of 33 km. In this area, the perpendicular profile CEL10 of the CELEBRATION 2000 experiment (Hrubcová *et al.* 2008) shows a gradient zone with velocities of 6.9–7.4 km s^{-1} in a depth range of 26–36 km. This gradient zone was interpreted along the whole eastern edge of the Bohemian Massif (profile CEL10), where strong lower crustal reflectivity with a long coda and weak *PmP* phases with unusually high apparent velocity suggested its existence. A slightly different character of the wavefield in the CEL10 data suggested differences between the Moravian and Silesian units. While in the Moravian part in the SW, the gradient zone has no distinct velocity contrast either at the top or bottom, more to the NE, in the Silesian unit, the *PmP* is more pronounced, although it is usually not the strongest reflection and is masked by reflections from the top of the lower crust.

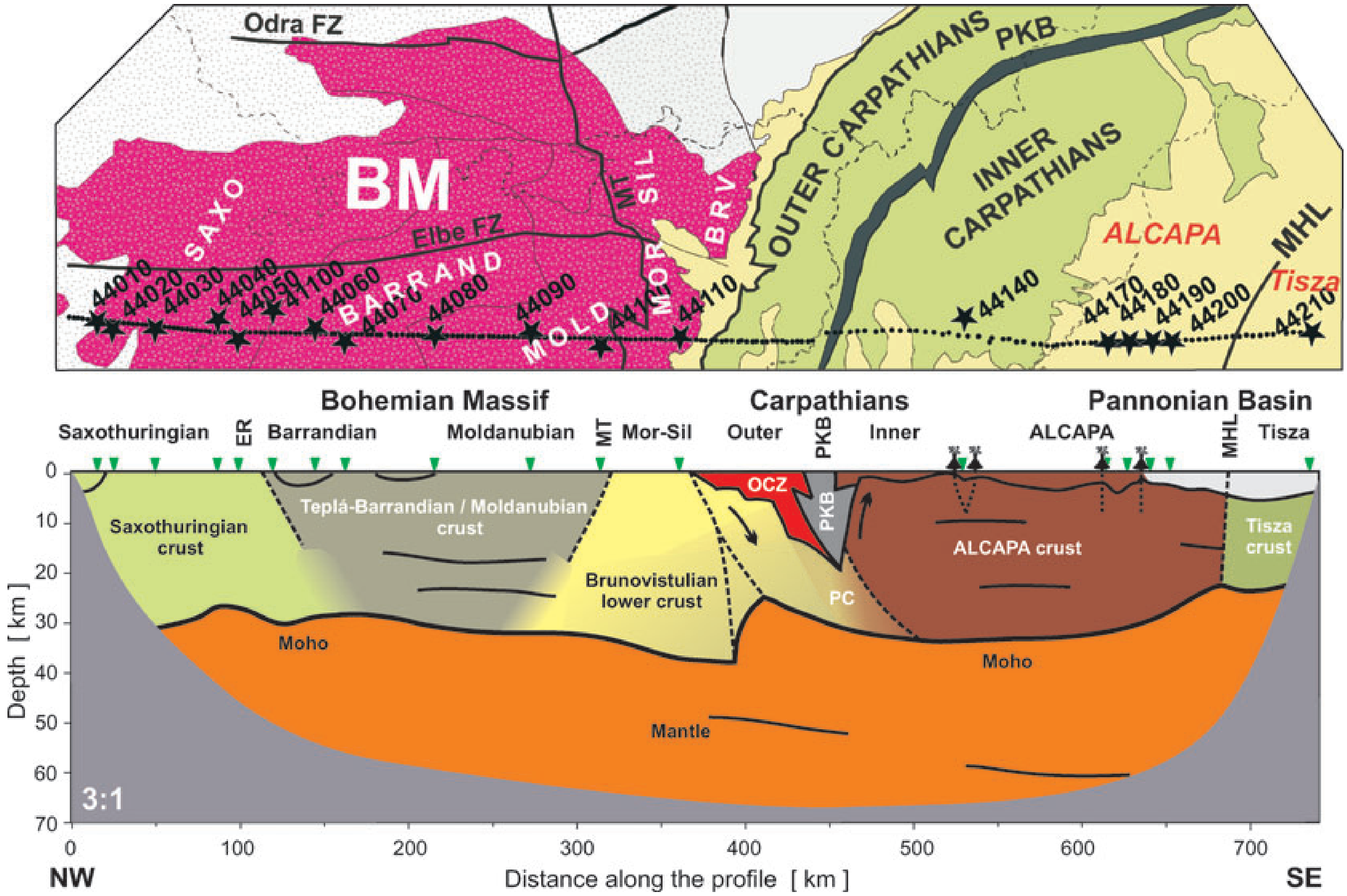

Figure 14. Schematic sketch indicating possible tectonic development along the S04 profile with surface geological map on the top. Vertical exaggeration is 3:1. SAXO, Saxothuringian; BARRAND, Barrandian; MOLD, Moldanubian; MT, Moldanubian Thrust; Mor-Sil, Moravo-Silesian; ER, Eger Rift; PKB, Pieniny Klippen Belt; OCZ, Outer Carpathians Zone; MHL, Mid-Hungarian Line; PC, Pieniny crust. The subdivision into the Outer Carpathians, the Pieniny Klippen Belt and the Pieniny crust is based on the results of reflection seismics (Tomek & Hall 1993) and geological interpretation (Vozár *et al.* 1999; Golonka & Krobicki 2004).

The Moravo-Silesian unit as a narrow SW-NE-trending zone of sheared and metamorphosed rocks was formed during the imbrication of the Brunovistulian. The S04 profile intersects it perpendicularly close to the contact of the Moravian and Silesian units. With the S04 data it is not possible to distinguish which of the aforementioned interpretations is more reliable. The traveltime residuals, as well as the synthetics for both cases show similar responses (Fig. 8). From the gravity modelling, the lower crust at the eastern side of the Bohemian Massif along the S04 profile can be modelled by slightly higher densities than those which ensue from seismic velocities, but not high enough to correspond to the high-velocity zone along the perpendicular CEL10 profile. For all these reasons it might be better to keep the simpler interpretation with the Moho as a first-order discontinuity, although a gradient zone can still be open to debate.

8.4 Tectonic development of the transition between the Bohemian Massif and the Carpathians

The area at the contact of the Bohemian Massif and the Carpathians is unique, because it represents tectonic development through three orogenic cycles (Grygar *et al.* 2002). The oldest cycle is the Cadomian orogeny, which led to the formation of the Brunovistulian unit. The second cycle, the Variscan orogeny, created the accretionary wedge, represented by the volcano-sedimentary formations of the Rhenohercynian Foredeep and the Sub-Variscan foreland. Finally, sequences of the West Carpathian Foredeep and the Outer West Carpathian nappes formed the Alpine accretionary wedge. The Brunovistulian is the oldest crustal segment and represents a foreland of both the above-mentioned accretionary wedges: the older Variscan one with generally NE directed kinematics and the younger Alpine wedge with northward tectonics.

The Moho in this area features strong lateral variations in a depth range of 26–37 km. It is constrained by the refraction from the upper mantle and shows an abrupt change from a depth of 26 km at a distance of 415 km followed by a steeply dipping portion to a depth of 37 km in a distance range of 390–415 km. Bielik *et al.* (2006) discuss the tectonic position of the Brunovistulian upper crust subducted into the lower-crustal position beneath the accretionary wedge. Slightly elevated seismic velocities of 6.6–6.75 km s^{-1} compared to the Moldanubian with velocities of 6.4 km s^{-1} can represent the extent of the Brunovistulian lower crust underthrust beneath the Moravo-Silesian.

8.5 Tectonic development of the Western Carpathians

The crust of the Western Carpathians has a complicated structure and is composed of fragments formed during the Variscan, paleo-Alpine and neo-Alpine orogenic events (McCann 2008b). The S04 profile is in a favourable position and cuts all main tectonic units of the Western Carpathians. At 400 km along the profile, it reaches the sedimentary infill (velocities of ∼4 km s^{-1} to a depth of 6 km) of the Carpathian Foredeep forming a characteristic clastic wedge thinning towards the foreland, followed by the Tertiary accretionary complex, the Carpathian Flysch Belt. This corresponds to the pronounced gravity low in the Carpathians. However, during modelling it was necessary to introduce lower densities of 2.45 g cm^{-3} than those which ensued from the velocity-to-density conversion (2.5 g cm^{-3}). The local gravity minimum at a distance of 425 km (densities of 2.2 g cm^{-3}) represents light Neogene to Quaternary sedimentary rocks of the Vienna basin margins, not distinguishable in the seismic data because of the larger distance to the nearest shot points in this area.

The Inner Western Carpathians are composed of tectonic units that originated during the paleo-Alpine Orogeny in the Mesozoic. They comprise numerous nappes composed of low- to high-grade metamorphic and plutonic Palaeozoic rocks and largely unmetamorphosed Palaeozoic to Cretaceous strata, which in the area of our investigation are largely north-west verging. Lower velocities of 3.9 km s^{-1} at about 460 km along the profile reflect the Neogene to Quaternary sediments of the Pannonian Basin margin. Increased velocities of 5.8–5.9 km s^{-1} further to the SE represent the core mountains (Považský Inovec and Tríbeč) composed of pre-Alpine basement and its Mesozoic sedimentary cover. Higher velocities (5.6–5.8 km s^{-1}) of the andesitic and rhyolitic rocks of the Tertiary volcanic edifices (Štiavnica stratovolcano) are reached at 520–545 km, followed by the volcano-sedimentary complexes to a distance of 560 km. Elevated velocities at a distance of 610–650 km along the profile represent the western slopes of a Tertiary volcanic complex in northern Hungary (Matra stratovolcano) with mainly andesitic volcanism of the Miocene age (Seghedi *et al.* 2004). This is in agreement with the geological interpretation along the MT-15 profile (Vozár, personal communications).

The Jurassic/Cretaceous limestones of the Pieniny Klippen Belt (PKB) separating the Outer and Inner Carpathians are the important first-order tectonic structure in the Western Carpathians and can be found at about 450 km along the profile; however, this structure is not obvious in the S04 refraction data at the surface. It represents the contact of the Western Carpathian Internides and the stable European Platform, separating this platform from the microplate ALCAPA in the eastern segment. The abrupt change of the crustal thickness and the dipping Moho (from 37 to 26 km depth at a distance of 400 km along the profile) may represent the contact of these plates at the lower crustal level.

Such a change in crustal thickness is not unusual in the Carpathian crustal structure. A similar effect was modelled along the SW–NE oriented profile CEL11 (Janik *et al.* 2010) at the eastern edge of the Carpathians. Also, Hauser *et al.* (2007) detected the same structure at the south-eastern edge of the Carpathian Belt in Vrancea, the region of deeper seated present-day seismicity (Wenzel *et al.* 2002). Although not deep, the seismicity along the Peripieninic lineament, PKB (e.g. the area of Dobrá Voda, Kováč *et al.* 2002), indicates geotectonic activity at the western edge of the Western Carpathians.

Considering the Pieniny Klippen Belt as a deep-seated boundary between the colliding Palaeozoic lithospheric plate and the microplate ALCAPA, the zone of the abrupt Moho depth change can represent the continuation of this boundary to depth. Vozár *et al.* (1999) interpreted the Pieniny Klippen Belt, forming the dominant structures of the Western Carpathians, as subvertical flower structures reaching a depth of 12 km, possibly extending to a depth of about 16–17 km (Vozár, personal communication). The basement of the Pieniny Klippen Belt reflects the Jurassic-Cretaceous development (see, e.g. Golonka & Krobicki 2004) and is interpreted as the Pieniny crust. It is presented as an individual Pieniny terrane forming a part of the ALCAPA foredeep with an independent tectonic history during the Alpine orogeny (Janik *et al.* 2010).

Considering the larger distance between the nearest shot points (SP 44110 at the eastern edge of the Bohemian Massif and SP 44140 in the Carpathians), the seismic data in this area were not sufficient to constrain the surface structure, the exact shape and the position of the individual units at depth. The subdivision into the Outer Carpathians, the Pieniny Klippen Belt and the Pieniny crust, marked in Fig. 14, is based on the results from reflection seismic interpretation (Tomek & Hall 1993; Hubatka & Švancara 2002) and geological interpretation (e.g. Vozár *et al.* 1999; Golonka & Krobicki 2004).

The crustal thickness and the Moho depth in the Carpathian region clearly tend to decrease from west to east. The Western Carpathians are characterized by crustal thicknesses of 32–33 km, while in the regions influenced by Tertiary extension such as the Pannonian Basin the Moho rises up to a depth of 25 km. This is in agreement with the reflection seismic results (Tomek 1993; Tomek & Hall 1993), as well as the investigations of Bielik *et al.* (2004) who modelled the Pannonian gravity high. However, such thicknesses are small in comparison to those of many other orogens, for example in the Alps (Brückl *et al.* 2007). Based on gravity observations, Lillie *et al.* (1994) suggests that collision stopped at an early stage in the Western Carpathians while the collision in the Eastern Alps progressed to an advanced stage such that the orogen is underlain by the full thickness of the European continental crust.

Two SE-dipping mantle reflectors within a depth range of 50–60 km are documented below the Carpathians. In the Pannonian Basin, Posgay *et al.* (1981) interpreted a low-velocity layer in the upper mantle, the top of which is at a depth of 55 km. Because the lithosphere in the Pannonian Basin is quite thin, they suggest that the top of this layer is associated with the lithosphere–asthenosphere boundary. The SE mantle reflector modelled from the S04 seismic data cannot contribute to such a discussion as it is constrained by only a few shot points and is not resolved under the Pannonian Basin. The shallower mantle reflector, more to the NW close to the contact with the Bohemian Massif, cannot be associated with such a boundary because the lithosphere deepens towards the Bohemian Massif (e.g. Bielik *et al.* 2004).

9 SUMMARY AND CONCLUSIONS

The SUDETES 2003 profile S04 was designed to study the main features from the Variscan to the Tertiary, represented by the Bohemian Massif and the Western Carpathians. The S04 seismic model (Fig. 5) reveals a diverse and complex structure not only within the tectonic units, but also at their contacts (Fig. 14). The differences in seismic velocities can reflect, to some extent, the structural variances and tectonic events. The main features of the interpretation are summarized below and we hope that these results will be the basis for further integrated geophysical and tectonic analyses.

1. In the Bohemian Massif, the Saxothuringian shows higher near-surface velocities represented by the Palaeozoic metamorphic rocks compared to lower velocities at the contact of the Saxothuringian and Barrandian caused by low-density granites. The contrast is even more pronounced in densities than in seismic velocities suggesting deeper seated granites than ensue from seismic modelling.

2. The lower crust under the Saxothuringian exhibits a complicated structure. The allowable models range from a higher velocity

lower crust, double Moho or, as in the S04 final interpretation, the Moho with a velocity contrast with some lateral topography. As such, it reveals that the northern termination of the Saxothuringian is not a simple structure.

3. The major crystalline segment within the Bohemian Massif, the Moldanubian, shows velocities representing the metamorphic rocks exposed at the surface. The Moho is modelled as a first-order discontinuity, the depth of which is slightly shallower (33 km) at the northern rim of the Moldanubian compared to the central part of the Moldanubian in the Bohemian Massif with a depth of 39 km.

4. Compared to the Moldanubian unit, the lower crust under the Moravo-Silesian displays slightly elevated velocities (6.6–6.75 km s^{-1}) though the area is not modelled by a gradient zone as in the case of the perpendicular profile CEL10 along the eastern edge of the Bohemian Massif. Also gravity modelling does not confirm the gradient zone at lower crustal levels. The slightly elevated seismic velocities of the Moravo-Silesian unit can represent the extent of the Brunovistulian lower crust underthrust beneath the Moravo-Silesian.

5. At the contact of the Bohemian Massif with the Western Carpathians, the Moho depth shows strong lateral variations. Proceeding from the SE, at the western side of the Carpathians, the Moho rises from 32 km to a depth of 26 km at a distance of 415 km along the profile and steeply dips to the NW to a depth of 37 km. Such a steeply dipping Moho was also modelled along the SW–NE oriented profile CEL11 at the eastern edge of the Carpathians or at the south-eastern edge of the Carpathian Belt in Vrancea (Janik *et al.* 2010; Hauser *et al.* 2007).

6. Considering the Pieniny Klippen Belt as a deep-seated boundary between the colliding Palaeozoic lithospheric plate and the ALCAPA microplate, the abrupt change of the crustal thickness can represent the continuation of this boundary to depth. The close later proximity (<50 km) between these two significant crustal features (PKB and the abrupt Moho depth change) may suggest that the zone between them is an area of the contact of the European Platform plate and the microplate. This possibility needs further investigation because of its implications for the nature of this plate boundary.

7. In the Carpathians, lower velocities of 4 km s^{-1} to a depth of 6 km represent the sedimentary infill of the Carpathian Foredeep and Flysch thinning towards the foreland, which is a source of a pronounced gravity low.

8. Further to the SE, in the Carpathians, higher near-surface velocities correspond to the Tertiary volcanic complexes exposed at the surface.

9. The Moho in the Carpathians reaches a depth of 32–33 km. This relatively small thickness compared to those of many other orogens, e.g. the Alps, reflects a different tectonic evolution of the Carpathians with the internal Carpathians being parts of two consolidated paleo-Alpine lithospheric fragments or microplates Alcapa and Tisza.

10. In contrast, in the region influenced by Tertiary extension, in the Pannonian Basin, the Moho rises up to a depth of 25 km, which corresponds to the Pannonian gravity high and the Pannonian lithospheric thinning.

ACKNOWLEDGMENTS

The authors thank the SUDETES 2003 Working Group, which in addition to the authors, comprises: M. Behm, T. Bodoky, R. Brinkmann, M. Brož, E. Brückl, W. Czuba, T. Fancsik, B. Forkmann, M. Fort, E. Gaczyński, R. Greschke, S. Harder, A. Hemmann, T. Janik, G. Jentzsch, G. Kaip, G. R. Keller, K. Komminaho, M. Korn, O. Karousová, M. Majdański, J. Málek, M. Malinowski, K. C. Miller, E.-M. Rumpfhuber, A. Špičák, E. Takács, T. Tiira, M. Wilde-Piórko, J. Yliniemi and A. Żelaźniewicz. It is only through the participation of approximately 200 individuals that the preparation, execution, and data processing for SUDETES 2003 could be successfully completed. The University of Leipzig provided 25 instruments for this project. Sources of financial and infrastructure support are in Austria, Institute of Geodesy and Geophysics, Vienna University of Technology; in Czech Republic, Ministry of Environment of the Czech Republic; and in Finland, Finnish participation was based on a long-standing exchange between the Finnish and Polish Academies of Sciences; in Germany, German participation was supported by the Friedrich-Schiller-Universität, Jena and the Bundesanstalt für Geologie Wissenschaften und Rohstoffe; in Hungary, Eötvös Loránd Geophysical Institute; in Poland, Polish Oil and Gas Company, and Institutes of Geophysics of the Polish Academy of Sciences and the University of Warsaw through the Association for Deep Geological Investigations in Poland (ADGIP); in Slovak Republic, the Geological Survey and Academy of Sciences provided support; in the United States, direct funding was provided by the National Science Foundation (NSF) and the Texas Higher Education Coordinating Board. IRIS/PASSCAL is supported by the U.S. National Science Foundation (NSF) and provided the majority of the instrumentation for this experiment, and most of these instruments were provided through grants to the University of Texas at El Paso (State of Texas Higher Education Coordinating Board, NSF/MRI, and the DOD). The work was also supported by the Grant Agency of the Czech Republic, grant P210/10/2063. The authors are grateful to G. Randy Keller and anonymous reviewers for valuable comments that improved the paper.

REFERENCES

Behr, H.J., Dürbaum, H.J. & Bankwitz, P. (Eds.), 1994. Crustal structure of the Saxothuringian zone: results of the deep seismic profile MVE-90 (East), *Z. Geol. Wiss.,* **22,** 647–769.

Beránek, B. & Zátopek, A., 1981. Earth's crust structure in Czechoslovakia and central Europe by methods of explosion seismology, in *Geophysical Synthesis in Czechoslovakia,* pp. 253–264, ed. Zátopek, A., Veda, Bratislava, Slovakia.

Beránek, B. & Zounková, M., 1977. Investigations of the Earth's crust in Czechoslovakia using industrial blasting, *Stud. Geophys. Geod.,* **21,** 273–280.

Bielik, M. *et al*., 2006. Gravity anomaly map of the CELEBRATION 2000 region, *Geologica Carpathica,* **57**(3), 145–156.

Bielik, M., Šefara, J., Kováč, M., Bezák, V. & Plašienka, D., 2004. The Western Carpathians—interaction of Hercynian and Alpine processes, *Tectonophysics,* **393,** 63–86.

Birkenmajer, K., 1986. Stages of structural evolution of the Pieniny Klippen Belt, Carpathians. *Stud. Geol. Pol.,* **88,** 7–32.

Blecha, V., Štemprok, M. & Fischer, T., 2009. Geological interpretation of gravity profiles through the Karlovy Vary granite massif (Czech Republic), *Stud. geophys. Geod.,* **53,** 295–314.

Brückl, E. *et al*., 2003. ALP 2002 seismic experiment, *Stud. geophys. Geod.,* **47,** 71–679, doi:10.1023/A:1024780022139.

Brückl, E. *et al*., 2007. Crustal structure due to collisional and escape tectonics in the Eastern Alps region based on profiles Alp01 and Alp02 from the ALP 2002 seismic experiment, *J. geophys. Res.,* **112,** B06308, doi:10.1029/2006JB004687.

Bucha, V. & Blížkovský, M. (Eds.), 1994. *Crustal Structure of the Bohemian Massif and the West Carpathians,* Academia Praha, Prague.

Čermák, V., 1995. A geothermal model of the Central Segment of the European Geotraverse, *Tectonophysics,* **244,** 51–55.

Červený, V. & Pšenčík, I., 1984. SEIS83—numerical modelling of seismic wave fields in 2-D laterally varying layered structures by the ray method. in

Documentation of Earthquake Algorithms, pp. 36–40, ed. Engdal, E.R., World Data Cent. A for Solid Earth Geophysics, Boulder, Colo, Rep. SE-35.

Christensen, N.I., 1974. Compressional wave velocities in possible mantle rocks to pressures of 30 kbars, *J. geophys. Res.,* **79,** 407–412.

Christensen, N.I. & Mooney, W.D., 1995. Seismic velocity structure and composition of the continental crust: a global view, *J. geophys. Res.,* **100**(B6), 97619788, doi:10.1029/95JB00259.

Dallmeyer, D., Franke, W. & Weber, K. (Eds.), 1995. *Pre-Permian Geology of Central and Eastern Europe,* Springer-Verlag, New York.

DEKORP Research Group, 1994. The deep seismic reflection profiles DEKORP 3/MVE-90, *Z. Geol. Wiss.,* **22**(6), 623–825.

Downes, H., 1993. The nature of the lower continental crust of Europe: petrological and geochemical evidence from xenoliths, *Phys. Earth planet. Int.,* **79,** 195–218.

Dudek, A., 1980. The crystalline basement block of the Outer Carpathians in Moravia, Bruno-Vistullicum, Rozpr. Čs. Acad. Věd, Prague.

Embey-Isztin, A., Downes, H., Kempton, P.D., Dobosi, G. & Thirwall, M., 2003. Lower crustal granulite xenoliths from the Pannonian Basin, Hungary. Part 1. Mineral chemistry, thermobarometry and petrology, *Contrib. Mineral. Petrol.,* **144,** 652–670.

Emmermann, R. & Lauterjung, J., 1997. The German Continental Deep Drilling Program KTB: overview and major results, *J. geophys. Res*., **102**(B8), 18 179–18 201.

Enderle, U., Schuster, K., Prodehl, C., Schulze, A. & Bribach, J., 1998. The refraction seismic experiment GRANU95 in the Saxothuringian belt, southeastern Germany, *Geophys. J. Int.,* **133,** 245–259, doi:10.1046/j.1365-246X.1998.00462.x.

Golonka, J. & Krobicki, M., 2004. Jurassic paleogeography of the Pieniny and Outer Carpathian basins, *Riv. It. Pal. strat.,* **110,** 5–14.

Grad, M., Keller, G.R., Thybo, H., Guterch, A. & the POLONAISE Working Group, 2002. Lower lithospheric structure beneath the Trans European Suture Zone from POLONAISE'97 seismic profiles, *Tectonophysics,* **360,** 153–168, doi:10.1016/S0040-1951(02)00350-5.

Grad, M. *et al*., 2003a. Crustal structure of the Trans-European suture zone region along POLONAISE'97 seismic profile P4, *J. geophys. Res.,* **108**(B11), 2541, doi:10.1029/2003JB002426.

Grad, M., Špičák, A., Keller, G.R., Guterch, A., Brož, M., Hegedűs, E. & Working Group, 2003b. SUDETES 2003 seismic experiment, *Stud. geophys. Geod.,* **47,** 681–689, doi:10.1023/A:1024732206210.

Grad, M *et al*., 2006. Lithospheric structure beneath trans-Carpathian transect from Precambrian platform to Pannonian basin: CELEBRATION 2000 seismic profile CEL05, *J. geophys. Res.,* **111,** B03301, doi:10.1029/2005JB003647.

Grad, M., Guterch, A., Mazur, S., Keller, G.R., Špičák, A., Hrubcová, P. & Geissler, W.H., 2008. Lithospheric structure of the Bohemian Massif and adjacent Variscan belt in central Europe based on profile S01 from the SUDETES 2003 experiment, *J. geophys. Res.,* **113,** B10304, doi:10.1029/2007JB005497.

Grégoire, M., Jackson, I., O'Reilly, S.Y. & Cottin, J.Y., 2001. The lithospheric mantle beneath the Kerguelen Islands (Indian Ocean): petrological and petrophysical characteristics of mantle mafic rock types and correlation with seismic profiles, *Contrib. Mineral Petrol.,* **142,** 244–259.

Grygar, R., Gnojek, I., Hubatka, F. & Jelínek, J., 2002. Brunovistulian Terrane—synthesis of morphostructural analysis and geophysical data (Moravo-Silesian Area, Czech Republic), *Geolines,* **14,** 26–27.

Guterch, A., Grad, M., Thybo, H., Keller, G.R. & Miller, K.C., 1998. Seismic experiment spreads across Poland, Eos Trans, *AGU,* **79**(26), 302–305.

Guterch, A., Grad, M., Thybo, H., Keller, G.R. & the POLONAISE Working Group, 1999. POLONAISE'97—International seismic experiment between Precambrian and Variscan Europe in Poland, *Tectonophysics,* **314,** 101–121, doi:10.1016/S0040-1951(99)00239-5.

Guterch, A., Grad, M., Špičák, A., Brückl, E., Hegedűs, E., Keller, G.R., Thybo, H. & CELEBRATION 2000, ALP 2002, SUDETES 2003 Working Groups, 2003a. An overview of recent seismic refraction experiments in central Europe, *Stud. geophys. Geod.,* **47,** 651–657, doi:10.1023/A:1024775921231.

Guterch, A. *et al*., & the CELEBRATION 2000 Experiment Team, 2003b. CELEBRATION 2000 seismic experiment, *Stud. geophys. Geod.,* **47,** 659–669, doi:10.1023/A:1024728005301.

Hauser, F., Raileanu, V., Fielitz, W., Dinu, C., Landes, M., Bala, A. & Prodehl, C., 2007. Seismic crustal structure between the Transylvanian Basin and the Black Sea, Romania, *Tectonophysics,* **430,** 1–25, doi:10.1016/j.tecto.2006.10.005.

Horváth, F., 1993. Towards a mechanical model for the formation of the Pannonian Basin, *Tectonophysics,* **226,** 333–357.

Hrubcová, P. & Geissler, W.H., 2009. The crust-mantle transition and the Moho beneath the Vogtland/West Bohemian Region in the light of different seismic methods, *Stud. geophys. Geod.,* **53,** 275–294,

Hrubcová, P., Środa, P. & CELEBRATION 2000 Working Group, 2008. Crustal structure at the easternmost termination of the Variscan belt based on CELEBRATION 2000 and ALP 2002 data, *Tectonophysics,* **460,** 55–75, doi:10.1016/j.tecto.2008.07.009.

Hrubcová, P., Środa, P., Špičák, A., Guterch, A., Grad, M., Keller, R.G., Brückl, E. & Thybo, H., 2005. Crustal and uppermost mantle structure of the Bohemian Massif based on data from CELEBRATION 2000 experiment. *J. geophys. Res.,* **110,** B11305. doi:10.1029/2004JB003080.

Hubatka, F. & Švancara, J., 2002. *Geologicko-geofyzikální model zemské kůry v místě křížení profilů 8HR/85 a CEL10. Internal Report,* Archive of the Geophysical Institute ASCR, Czech.

Janik, T. *et al*., & CELEBRATION 2000 Working Group, 2010. Crustal structure of the Western Carpathians and Pannonian Basin System: seismic models from CELEBRATION 2000 data and geological implication, *J. Geodyn.,* in press.

Janočko, J. & Jacko, S., 1999. Evolution of the Central Paleogene Basin in the Spiska Magura region, Slovakia, *Geologica Carpathica,* **50,** 36–37.

Kempton, P.D., Downes, H. & Embey-Isztin, A., 1997. Mafic granulite xenoliths in Neogene alkali basalts from the western Pannonian Basin: insights into the lower crust of a continental back-arc setting, *J. Petrol.,* **38,** 941–970.

Komminaho, K., 1997, *Software Manual for Programs MODEL and XRAYS—A Graphical Interface for SEIS83 Program Package, Report 20, 31,* Department of Geophysics University of Oulu, Oulu, Finland.

Konečný, V., Kováč, M., Lexa, J., & Šefara, J., 2002. Neogene evolution of the Carpatho-Pannonian region. An interplay of subduction and back-arc diapiric uprise in the mantle, *EGS Stefan Mueller Special Publication Series,* **1,** 165–194.

Kopecký, L., 1978. Neoidic taphrogenetic evolution and young alkaline volcanism of the Bohemian Massif, Czech Geological Survey, *Geology,* **31,** 91–107.

Kováč, M. *et al*., 2002. Seismic activity and neotectonic evolution of the Western Carpathians (Slovakia), *EGU Stephan Mueller Spec. Publ. Ser.,* **3,** 167–184.

Krzywiec, P., 1997. Large-scale tectono-sedimentary Middle Miocene history of the central and eastern Polish Carpathian Foredeep Basin—results of seismic data interpretation, *Przeglad Geologiczny,* **45,** 1039–1053.

Lenhardt, W.A., Švancara, J., Melichar, P., Pazdírková, J., Havíř, J. & Sýkorová, Z., 2007. Seismic activity of the Alpine-Carpathian-Bohemian Massif region with regard to geological and potential field data, *Geol. Carpathica,* **58,** 397–412.

Lillie, J.R., Bielik, M., Babuška, V. & Plomerová, J., 1994. Gravity modelling of the lithosphere in the Eastern Alpine–Western Carpathian–Pannonian Basin region, *Tectonophysics,* **231,** 215–235.

Ludwig, W.J., Nafe, J.E. & Drake, C.L., 1971. Seismic refraction, in *The Sea,* Vol. 4, pp. 53–84, ed. Maxwell, A.E., Interscience, New York.

Majdański, M., Grad, M., Guterch, A. & SUDETES 2003 Working Group, 2006. 2-D seismic tomographic and ray tracing modelling of the crustal structure across the Sudetes Mountains basing on SUDETES 2003 experiment data, *Tectonophysics,* **413,** 249–269, doi:10.1016/j.tecto.2005.10.042.

Majdański, M., Kozlovskaya, E., Grad, M. & SUDETES 2003 Working Group, 2007. 3D structure of the Earth's crust beneath the northern part of the Bohemian Massif, *Tectonophysics,* **437,** 17–36, doi:10.1016/j.tecto.2007.02.015.

Majerová, M. & Novotný, M., 1986, Výzkum zemské kůry pomocí hlubinné sondáže, in ed. Blížkovský, M., *Geofyzikální model litosféry, MS Geofyzika n.p. Brno, GFÚ ČSAV Praha,* GFÚ SAV Bratislava, Czech.

Majorowicz, J., 1976. Heat flow map of Poland on the background of geothermal field of Europe and some aspects of its interpretation, *Acta geophys. Polonica, 24*, 147–156.

Málek, J., Brož, M., Fischer, T., Horálek, J., Hrubcová, P., Janský, J., Novotný, O. & Růžek, R., 2001. Seismic measurements along short profiles in Western Bohemia during the CELEBRATION 2000 experiment, *Acta Montana, Ser. A,* **18,** 15–28.

Malinowski, M., Żelaźniewicz, A., Grad, M., Guterch, A., Janik, T. & CELEBRATION Working Group, 2005. Seismic and geological structure of the crust in the transition from Baltica to Palaeozoic Europe in SE Poland–CELEBRATION 2000 experiment, profile CEL 02, *Tectonophysics,* **401**(1–2), 55–77.

Malinowski, M., Grad, M., Guterch, A. & the CELEBRATION 2000 Working Group, 2008. 3-D seismic modelling of the crustal structure between East European craton and the Carpathians in SE Poland based on CELEBRATION 2000 data, *Geophys. J. Int.,* **173,** 546–565, doi:10.1111/j.1365-246X.2008.03742.x.

Matte, P., Maluski, H., Rajlich, P. & Franke, W., 1990. Terrane boundaries in the Bohemian Massif: result of large-scale Variscan shearing, *Tectonophysics,* **177,** 151–170, doi:10.1016/0040-1951(90)90279-H.

Matte, Ph., 1991. Accretionary history and crustal evolution of the Variscan belt in Western Europe, *Tectonophysics,* **196,** 309–337.

Matte, Ph., 2001. The Variscan collage and orogeny (480–290 Ma) and the tectonic definition of the Armorica microplate: a review, *Terra Nova,* **13,** 122–128.

McCann, T. (Ed.), 2008a. *The Geology of Central Europe. Volume 1: Precambrian and Palaeozoic,* Geological Society, London.

McCann, T. (Ed.), 2008b. *The Geology of Central Europe. Volume 2: Mesozoic and Cenozoic,* Geological Society, London.

Mlčoch, B., 2001. Výzkum krystalických formací v hlubokých strukturách Doupovského komplexu a jeho širšího okolí, Český geologický ústav, Final report, Czech.

Mueller, H.J., 1995. Modelling of the lower crust by simulation of the in situ conditions: an example from Saxonian Erzgebirge, *Phys. Earth planet. Inter.,* **92,** 3–15.

Plašienka, D., Grecula, P., Putiš, M., Hovorka, D. & Kováč, M., 1997. Evolution and structure of the Western carpathians: an overview, in *Geological Evolution of the Western Carpathians,* eds Grecula, P., Hovorka, D. & Putiš, M., Geocomplex, Bratislava.

Posgay, K., Albu, I., Petrovics, I. & Ráner, G., 1981. Character of the Earth's crust and upper mantle on the basis of seismic reflection measurements in Hungary, *Earth Evol. Sci.,* **1,** 272–279.

Posgay, K., Albu, I., Ráner, G. & Varga, G., 1986. Characteristics of the reflecting layers in the Earth's crust and upper mantle in Hungary, in *Reflection Seismology: A Global Perspective,* Vol. 13, pp. 55–66, eds Barazangi, M. & Brown, L., Geodynamics Series, AGU, Washington, DC.

Posgay, K. *et al*., 1995. Asthenospheric structure beneath a Neogene Basin in SE Hungary, *Tectonophysics,* **252,** 467–484.

Posgay, K., Fancsic, T., Hegedűs, E., Pápa, A., Bodoky, T. & Takács, E., 2001. Metamorphic and geologic effects shown by seismic data in the Carpathian Basin, *Acta Geol. Hungarica,* **44,** 113–134.

Prodehl, C., Mueller, S. & Haak, V., 1995. The European cenozoic rift system, in *Continental Rifts: Evolution, Structure, Tectonics, Development of Geotectonics,* Vol. 25, pp. 133–212, ed. Olsen, K.H., Elsevier, New York.

Reicherter, K. *et al*., 2008. Alpine tectonics north of the Alps, in *The Geology of Central Europe. Volume 2: Mesozoic and Cenozoic,* pp. 1233–1285, ed. McCann, T., Geological Society, London.

Royden, L., Horváth, F. & Rumpler, J., 1983. Evolution of the Pannonian basin system, *Tectonics,* **2,** 63–90.

Růžek, B., Vavryčuk, V., Hrubcová, P., Zedník, J. & the CELEBRATION Working Group, 2003. Crustal anisotropy in the Bohemian Massif, Czech Republic: Observations based on Central European Lithospheric Experiment Based on Refraction (CELEBRATION) 2000, *J. geophys. Res.,* **108**(B8), 2392, doi:10.1029/2002JB002242.

Růžek, B., Hrubcová, P., Novotný, M., Špičák, A., & Karousová, O., 2007. Inversion of travel times obtained during active seismic refraction experiments Celebration 2000, Alp 2002 and Sudetes 2003, *Stud. geophys. Geod.,* **51,** 141–164, doi:10.1007/s11200-007-0007-6.

Šantavý, J. & Vozár, J., 2000. *Electronical Atlas of Deep Reflection Seismic Profiles of the Western Carpathians,* Ministery of Environment and Geological Survey of the Slovak Repubic, Geocomplex, Bratislava.

Schulmann, K. & Gayer, R., 2000. A model for a continental accretionary wedge developed by oblique collision: the NE Bohemian Massif, *J. Geol. Soc. Lond.* **157,** 401–416.

Schulmann, K., Kröner, A., Hegner, E., Wendt, I., Konopásek, J., Lexa, O. & Štipská, P., 2005. Chronological constraints on the pre-orogenic history, burial and exhumation of deep-seated rocks along the Eastern Margin of the Variscan Orogen, Bohemian Massif, Czech Republic, *Am. J. Sci.,* **305,** 407–448.

Seghedi, I., Downes, H., Vaselli, O., Szakacs, A., Balogh, K. & Pécskay, Z., 2004. Post-collisional Tertiary–Quaternary mafic alkalic magmatism in the Carpathian–Pannonian region: a review, *Tectonophysics,* **393,** 43–62, doi:10.1016/j.tecto.2004.07.051.

Soták, J., Pereszlenyi, M., Marchalko, R., Milicka, J. & Starek, D., 2001. Sedimentology and hydrocarbon habitat of the submarine-fan deposits of the Central Carpathian Paleogene Basin (NE Slovakia), *Marine Petroleum Geol.,* **18,** 87–114.

Środa, P. *et al*., & CELEBRATION 2000 Working Group, 2006. Crustal and upper mantle structure of the Western Carpathians from CELEBRATION 2000 profiles CEL01 and CEL04: seismic models and geological implications, *Geophys. J. Int.,* **167,** 737–760, doi:10.1111/j.1365-246X.2006.03104.x.

Tari, G., Báldi, T. & Báldi-Beke, M., 1993. Paleogene retroarc flexural basin beneath the Neogene Pannonian Basin: a geodynamic model, *Tectonophysics,* **226,** 433–455.

Taylor, S.R. & Toksöz, M.N., 1982. Crust and upper-mantle velocity structure in the Appalachian orogenic belt: implications for tectonic evolution, *Geol. Soc. Am. Bull.,* **93,** 315–329.

Tomek, Č., 1993. Deep crustal structure beneath the central and inner West Carpathians, *Tectonophysics,* **226,** 417–431.

Tomek, C. & Hall, J., 1993. Subducted continental margin imaged in the Carpathians of Czechoslovakia, *Geology,* **21,** 535–538.

Vavryčuk, V., Hrubcová, P., Brož, M., Málek, J. & the ALP 2002 Working Group, 2004. Azimuthal variation of Pg velocity in the Moldanubian, Czech Republic: observations based on a multi-azimuthal common-shot experiment, *Tectonophysics,* **387,** 189–203.

Villaseca, C., Downes, H., Pin, C. & Barbero, L., 1999. Nature and composition of the lower continental crust in Central Spain and the granulite-granite linkage: inferences from granulite xenoliths, *J. Petrol.,* **40,** 1465–1496.

Vosteen, H.-D., Rath, V., Clauser, C. & Lammerer, B., 2003. The thermal regime of the Eastern Alps from inversion analyses along the TRANSALP profile, *Phys. Chem. Earth,* **28,** 393–405.

Vozár, J. *et al*., 1999. *Atlas of Deep Reflection Seismic Profiles of the Western Carpathians and Their Interpretation,* Geological Survey of Slovak Republic, Bratislava.

Wedepohl, K.H., 1995. The composition of the continental crust, *Geochim. Cosmochim. Acta,* **59,** 1217–1232.

Weiss, T., Siegesmund, S., Rabbel, W., Bohlen, T. & Pohl, M., 1999. Seismic velocities and anisotropy of the lower continental crust: a review, *Pure appl. Geophys.,* **156,** 97–122.

Wenzel, F., Sperner, B., Lorenz, F. & Mocanu, V., 2002. Geodynamics, tomographic images and seismicity of the Vrancea region (SE-Carpathians, Romania), *EGU Stephan Mueller Spec. Publ. Ser.,* **3,** 95–104.

Zelt, C., 1994. *ZPLOT–An Interactive Plotting and Picking Program for Seismic Refraction Data, Report, Bullard Laboratory,* University of Cambridge, Cambridge, UK.

Zuchiewicz, W., Tokarski, A.K., Jarosiński, M. & Márton, E., 2002. Late Miocene to present day structural development of the Polish segment of the Outer Carpathians, *Stephan Mueller Spec. Publ. Ser.,* **3,** 185–202.